www.coinweb.no

SINTEF Building and Infrastructure Harald Justnes

Low porosity through optimized particle packing of concrete matrix

COIN Project report 13 - 2009

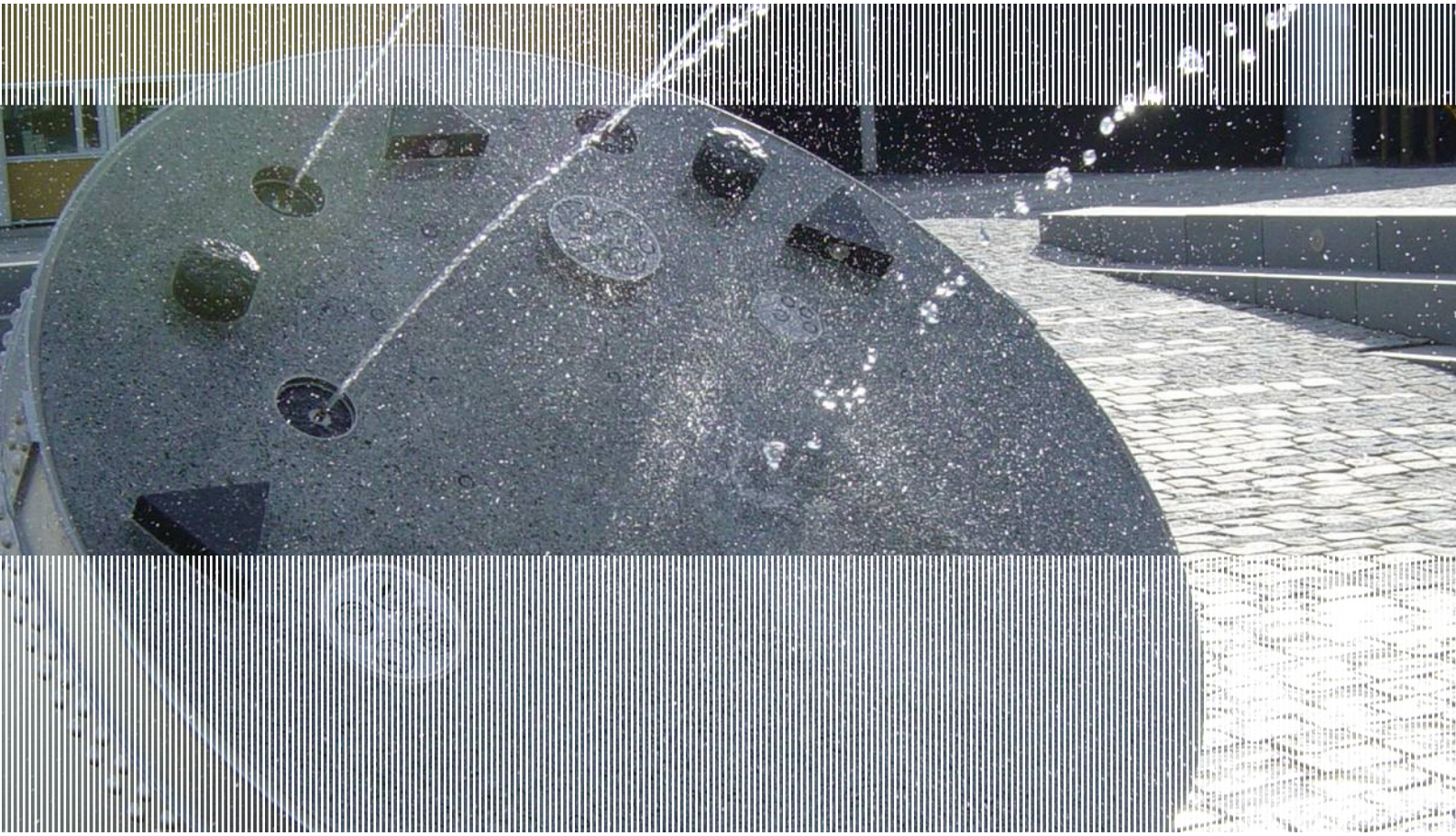

SINTEF

SINTEF Building and Infrastructure

Harald Justnes

Low porosity through optimized particle packing of concrete matrix

COIN P1 Advanced cementing materials and admixtures

SP 1.5 Low porosity/ permeability

COIN Project report 13 – 2009

COIN Project report no 13
Harald Justnes
Low porosity through optimized particle packing of concrete matrix
COIN P1 Advanced cementing materials and admixtures
SP 1.5 Low porosity/ permeability

Keywords:
Materials technology, concrete, porosity, permeability, particle packing

Photo, cover: «Reflection» by Kari Elise Mobeck

ISSN 1891–1978 (online)
ISBN 978-82-536-1096-2(pdf)

Address: Forskningsveien 3 B
POBox 124 Blindern
N-0314 OSLO
Tel: +47 22 96 55 55
Fax: +47 22 69 94 38 and 22 96 55 08

www.sintef.no/byggforsk
www.coinweb.no

Cooperation partners / Consortium Concrete Innovation Centre (COIN)

Aker Solutions
Contact: Jan-Diederik Advocaat
Email: jan-diederik.advocaat@akersolutions.com
Tel: +47 67595050

Borregaard Ligno Tech
Contact: Kåre Reknes
Email: kare.reknes@borregaard.com
Tel: +47 69118000

maxit Group AB
Contact: Geir Norden
Email: geir.norden@maxit.no
Tel: +47 22887700

Norcem AS
Contact: Terje Rønning
Email: terje.ronning@norcem.no
Tel: +47 35572000

NTNU
Contact: Terje Kanstad
Email: terje.kanstad@ntnu.no
Tel: +47 73594700

Rescon Mapei AS
Contact: Trond Hagerud
Email: trond.hagerud@resconmapei.no
Tel: +47 69972000

SINTEF Building and Infrastructure
Contact: Tor Arne Hammer
Email: tor.hammer@sintef.no
Tel: +47 73596856

Skanska Norge AS
Contact: Sverre Smeplass
Email: sverre.smeplass@skanska.no
Tel: +47 40013660

Spenncon AS
Contact: Ingrid Dahl Hovland
Email: ingrid.dahl.hovland@spenncon.no
Tel: +47 67573900

Norwegian Public Roads Administration
Contact: Kjersti K. Dunham
Email: kjersti.kvalheim.dunham@vegvesen.no
Tel: +47 22073940

Unicon AS
Contact: Stein Tosterud
Email: stto@unicon.no
Tel: +47 22309035

Veidekke Entreprenør ASA
Contact: Christine Hauck
Email: christine.hauck@veidekke.no
Tel: +47 21055000

Preface

This study has been carried out within COIN - Concrete Innovation Centre - one of presently 14 Centres for Research based Innovation (CRI), which is an initiative by the Research Council of Norway. The main objective for the CRIs is to enhance the capability of the business sector to innovate by focusing on long-term research based on forging close alliances between research-intensive enterprises and prominent research groups.

The vision of COIN is creation of more attractive concrete buildings and constructions. Attractiveness implies aesthetics, functionality, sustainability, energy efficiency, indoor climate, industrialized construction, improved work environment, and cost efficiency during the whole service life. The primary goal is to fulfil this vision by bringing the development a major leap forward by more fundamental understanding of the mechanisms in order to develop advanced materials, efficient construction techniques and new design concepts combined with more environmentally friendly material production.

The corporate partners are leading multinational companies in the cement and building industry and the aim of COIN is to increase their value creation and strengthen their research activities in Norway. Our over-all ambition is to establish COIN as the display window for concrete innovation in Europe.

About 25 researchers from SINTEF (host), the Norwegian University of Science and Technology - NTNU (research partner) and industry partners, 15 - 20 PhD-students, 5 - 10 MSc-students and a number of international guest researchers, work presently on 5 projects:

- Advanced cementing materials and admixtures
- Improved construction techniques
- Innovative construction concepts
- Operational service life design
- Energy efficiency and comfort of concrete structures

COIN has presently a budget of NOK 200 mill over 8 years (from 2007), and is financed by the Research Council of Norway (approx. 40 %), industrial partners (approx 45 %) and by SINTEF Building and Infrastructure and NTNU (in all approx 15 %).

For more information, see www.coinweb.no

Tor Arne Hammer
Centre Manager

Summary

This State-of-the-Art report (STAR) gives an overview over factors influencing particle packing and porosity. An overview of methods for measuring and modelling particle packing and porosity is also made. Improved particle packing of the concrete matrix (i.e. particles < 125 μm) will reduce porosity and permeability of concrete and thereby improve durability of concrete. The findings are based on literature reviews.

It appears like the fineness of the particles is determining the size of the pore openings governing the pore connectivity and thereby permeability if they are added in large enough quantities to disperse the coarser ones, which is obvious from basic particle packing theory. An excess of fine particles dispersing coarse ones (e.g. high dosage of silica fume relative to cement) can dominate the permeability all together, without being the result of a refined complex particle packing. For more normally distributed multiple particle compositions, a wider particle size distribution is more beneficial to obtain optimize particle packing.

It is also demonstrated that it is not only the initial packing of particles, but also the increased volume of their solid reaction products that reduces permeability. Even particles considered by many to be inert (like limestone powder) will react when given sufficient reactants (e.g. calcium alumina hydrates from pozzolanic reaction of fly ash) and theoretically contribute positively to reduced permeability.

Thus, making smallest possible *reacting* particles would give the ultimate low pore opening size. The challenge is to make them in the most economical way (grinding is expensive and limited to a certain size) and at the same time not let them hamper workability by being too reactive in the fresh state. Thus, the fine tail of particle size distributions of e.g. ternary cement should consist of slowly reacting particles; for instance nano-sized, precipitated calcium carbonate, clay calcined below sintering temperature easily ground to 3 μm or perhaps fine recycled glass powder. Further research is recommended along these lines.

It is also speculated whether initial Ettringite formation in fresh cement paste may hamper particle packing initially or not, and search for other setting regulators than gypsum may be a way to find this out. A gypsum free system may also allow high temperature curing and enable increased productivity. Future research should clarify this matter.

The most feasible way of determining particle packing in the fresh state seems to be a method called “centrifugal consolidation”, due to its simplicity, rapid result and operator independence.

Computer programs for calculating pore connectivity and permeability of hydrating cement paste is also reviewed and it seems that all programs suffer from the same problem; their resolution versus computing time. Many works with pixel values in excess of 1 μm and in concrete matrix there are many pores below this value that will not be predicted.

The most important parameters governing permeability and percolation of a concrete matrix seems to be pore connectivity and critical pore opening. There are indications showing that a concrete matrix will depercolate at a total porosity of 18-20 vol% independently of being obtained by low water-to-cement ratio, particle packing, degree of hydration etc.

When permeability of concrete matrix is lower than the whole concrete, it is pointed out that the permeability of the actual normal density aggregate may be higher than a well cured cementitious paste, and that the permeability increase observed for concrete not necessarily is due to a more porous interfacial zone between aggregate and matrix that many authors seem to focus on.

Table of contents

1 INTRODUCTION

1.1 Objective

This State-of-the-Art report (STAR) is meant to give an overview over how improved particle packing of the concrete matrix can reduce porosity and permeability of concrete.

The concrete matrix consist of all particles < 125 μm comprised of cement, supplementary cementing materials, fillers, fine sand etc. This STAR does therefore not treat particle packing of aggregates for concrete, which is a better known topic.

This STAR is no. 1 as described in the CTR of 2007 for activity 1.5f in COIN P1.

1.2 Background

Porosity and permeability of concrete is strongly related to its durability, since most aggressives will enter via the pore system. Reduced porosity and permeability will therefore mean a more durable concrete.

For instance are water born chlorides not harmful for the concrete matrix. However, when the concentration of chlorides becomes high enough at the reinforcing steel surface, corrosion will initiate formation of expansive corrosion products (rust) and eventually cracking of the concrete matrix when the stresses exceeds its tensile strength.

Likewise is carbonation by CO_2 from the air entering through the pores not detrimental for the concrete matrix. Carbonation will on the contrary slightly reduce the porosity of matrix due to the increase in solids volume (+15 vol%) by the process

$$Ca(OH)_2\,(s) + CO_2\,(aq) = CaCO_3\,(s) + H_2O. \qquad [1]$$

The conversion of calcium hydroxide to calcium carbonate will reduce the pH from 12.5 to about 8. Thus, when the carbonation front reaches the reinforcement steel, corrosion can start.

However, there are water born aggressives that are detrimental to the cement paste of the matrix that will enter through the pores. One example is sulphates that initially may form gypsum in reaction with calcium hydroxide and subsequently may form expansive Ettringite in reaction with various calcium aluminate hydrates inherent in the hydrated cement paste and lead to cracking. Even worse, if sufficient limestone (i.e. calcium carbonate) is added to the matrix, the binder CSH may combine with calcium carbonate and gypsum to the non-binding compound Thaumasite (Justnes, 2003) and the concrete loose its integrity all together (Justnes and Rodum, 2006).

The concrete matrix is strongly alkaline, and attack by even weakly acidic aggressives will therefore not depend on permeability but etch the matrix from the surface inwards.

Porosity will not only affect durability, but also the strength of the matrix, and development of ultra high strength cements often rely on optimized particle packing. Optimized particle packing can also improve rheology of the fresh matrix.

2 PRINCIPLES OF MATRIX POROSITY AND PERMEABILITY

2.1 Basic particle packing

If one considers monosized spheres (particles), they can pack to give cubic, octahedral or tetrahedral holes between them as illustrated in Figs. 1, 2 and 3, respectively.

The radius r_2 of a smaller sphere that can fit in the cubic hole of cubically packed monosized spheres with radius r_1 without moving them apart, can be derived from Fig. 1 using Pythagoras's sentence;

$$(2r_1)^2 + (\sqrt{2}\cdot 2r_1)^2 = (2r_1 + 2r_2)^2 \rightarrow (\sqrt{3}-1)\cdot r_1 = r_2 \rightarrow r_2/r_1 = (\sqrt{3}-1) = 0.73$$

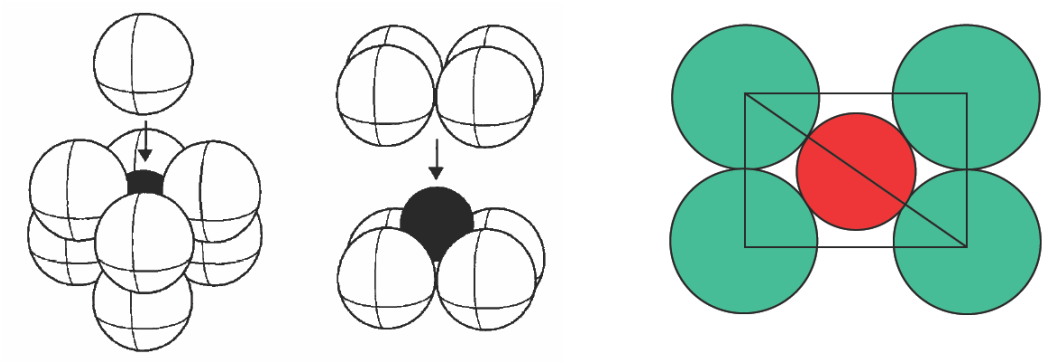

Fig. 1 Cubic packing (left and middle drawing). The far right drawing is a cross-sectional view of the cubic lattice along the face diagonal direction. For the rectangular unit cell, the length of the short axis is 2r (r is the radius of the large sphere), which also is the edge length of the cubic cell (middle drawing). The length of the long axis of the rectangular cell to the far right is $\sqrt{2}\cdot 2r$, which is the face diagonal of the cubic cell.

The radius r_3 of a smaller sphere that can fit in the octahedral hole of closest packed monosized spheres with radius r_1 without moving them apart, can be derived from Fig. 2 using Pythagoras's sentence;

$$(2r_1)^2 + (2r_1)^2 = (2r_1 + 2r_3)^2 \rightarrow (\sqrt{2}-1)\cdot r_1 = r_3 \rightarrow r_3/r_1 = (\sqrt{2}-1) = 0.41$$

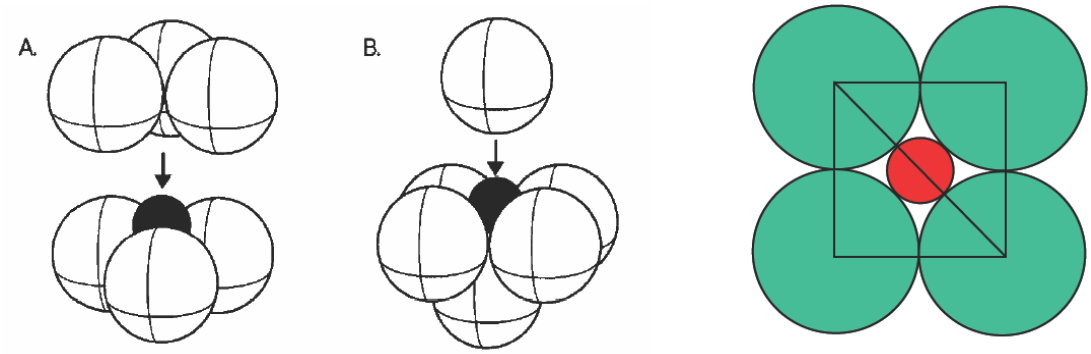

Fig. 2 Two views (A and B) of smaller sphere (black) in an octahedral hole formed by closest packing of larger spheres. The smaller sphere has physical contact with larger ones along the diagonal in the far left cross-sectional view.

In order to calculate the radius r_4 of a smaller sphere that can fit in the tetrahedral hole of closest packed monosized spheres with radius r_1 without moving them apart, one has to put the vertices of the tetrahedra at the four corners of a cube as shown to the far right of Fig. 3. The edge length of such a cubic cell will then be $a = 2r_1 \cdot \sin 45° = \sqrt{2} \cdot r_1$, while the body diagonal is $\sqrt{3} \cdot a = \sqrt{6} \cdot r_1$. Since the smaller and the large spheres are in contact along the body diagonal one have $2 \cdot (r_1 + r_4) = \sqrt{6} \cdot r_1 \rightarrow r_4/r_1 = \sqrt{6}/2 - 1 = 0.22$.

Wang et al (1997) studied the packing of two powders and found that the optimum ratio between the diameter of the two powders was 0.3, which happens to be the average diameter of smaller spheres fitting in octahedral (0.41) and tetrahedral (0.22) holes formed by closest packing of larger spheres of diameter 1.

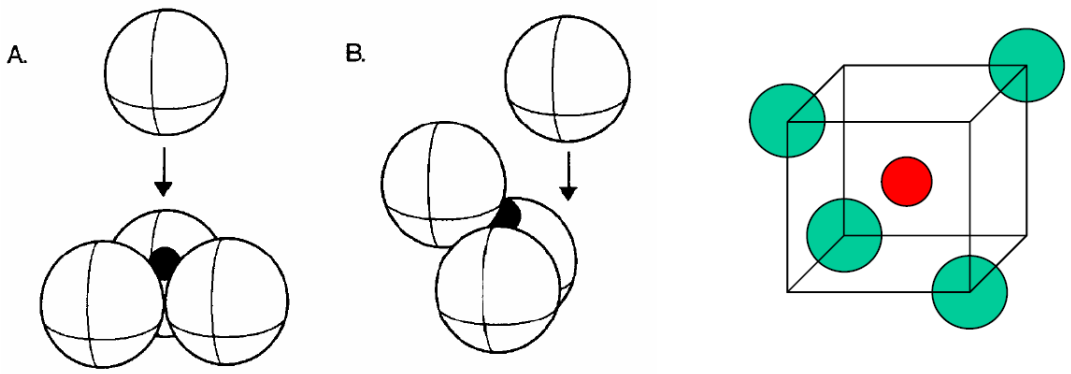

Fig. 3 Two views (A and B) of smaller sphere (black) in a tetrahedral hole formed by closest packing of larger spheres. The smaller sphere has physical contact with larger ones along the body diagonal of the cube drawn to the far right.

Note that a small sphere that are going to enter either an octahedral or a tetrahedral hole without disturbing the larger spheres must be smaller than the one that can fit into the holes. The entrance to the holes has the form of a triangle of equal sides with length $2r_1$ and fits a smaller sphere of radius r_2 according to Pythagoras's sentence

$$(r_1+r_5)^2/4 + r_1^2 = (r_1 + r_5)^2 \rightarrow r_5/r_1 = 2 \cdot (1 - \sqrt{3}/2)/\sqrt{3} = 0.15$$

If one considers these packing of spheres to be hardened cement grains and one wants to measure the pore size distribution by mercury intrusion porosimetry (MIP), it is easy to realize that one has to pressurize the mercury according to the smaller entrance to the hole. The larger hole fills then immediately since a lower mercury pressure is required. Thus, MIP really measures pore entries rather than pore sizes and this is what often is referred to as the "ink-bottle" effect, but since hardly anyone use "ink-bottles" anymore, the above illustration is perhaps just as good and will serve generations that have never seen an "ink bottle".

The preceding basic packing discussion can also serve as an indication on how polydisperse spherical particles can be optimally packed in theory. However, cement does not consist of spheres, but rather irregular, sharp-edged particles with a distribution of sizes.

It is important to notice that if large particles (e.g. cement) are dispersed in excess of smaller particles (e.g. silica fume), the voids between the packed smaller particles will dominate the pore sizes and the pore connectivity.

2.2 Porosity of matrix

One has to distinguish between total porosity and pore sizes. Total porosity is largely determined by the initial amount of water per volume unit and how much of it that is transferred to hydrates at any given time (e.g. degree of hydration for cement). Permeability is principally related to the total porosity as well as the pore sizes, tortuosity (i.e. actual connected pore length relative to thickness of sample) and degree of pore connectivity. Optimized particle packing will largely reduce the pore sizes and thereby permeability of a single pore and its tortuosity, while the nature of the particles (i.e. their reactivity and hydrates they form) also will influence the total porosity and thereby the connectivity of pores.

The porosity of cement extends over a wide range of length scales. Classically this is divided into:

- The so-called 'gel-pores' which are intrinsic to the CSH binder. This porosity lies in the range of a few nanometres and due to this small size plays only a minor role in transport processes affecting durability and other aspects of performance.
- Capillary pores corresponding to the originally water filled spaces not filled by hydration products. The size of these ranges from a few nanometres to tens of micrometers, i.e. more than 4 orders of magnitude (size depends probably on initial particle size and packing)
- The voids in hollow shells or the gaps between unreacted grains and C-S-H shells that are observed in cement pastes may also be considered as porosity although it is not clear to what extent these voids are connected to the capillary pore network.
- Air voids, from tens of μm to mm in size are heterogeneities of the original mix. They are a small fraction of the whole porosity but may interconnect capillary pores. However, they probably have a minor role in overall transport processes.

2.3 Pore connectivity (percolation and depercolation)

Pore connectivity (or percolation ability) is of importance for the permeability of cementitious materials. It is actually a complicated matter since it in addition to particle packing is a function of total porosity (largely governed by w/c) and degree of hydration and thereby time.

Cook and Hover (1999) studied cement paste with a number of different w/c at different curing times by mercury intrusion porosimetry (MIP) and concluded that the pores becomes discontinuous at a porosity of 18 vol% independently of the degree of hydration or w/c to achieve it.

Atahan et al (2009) recently discussed the effect of w/c and curing time on the *critical pore width* of hardened cement paste, a parameter they claimed could characterise the pore connectivity.

Ye (2005) made an excellent introduction to percolation that is partly referred here:
The percolation theory (Stauffer, 1992) deals with disordered multiphase media in which the disorder is characterized by the degree of connectivity of the phases. In percolation studies, one is often interested in the fraction of a phase that is connected across the microstructure as a function of the total volume of the phase (Bentz, 2000). The microstructure of cement-based materials provides numerous examples of percolation phenomena, such as percolation of the CSH and CH phases and percolation of the capillary pores phase (Bentz, 2000, Benz and Garboczi, 1991, and Ye et al (2004). In particular, the depercolation of the capillary pores is of great interest for studying the transport phenomena in cement-based materials. The application of the percolation theory for explaining the transport properties and, in particular, the permeability of cement-based materials can be summarized as follows. In the

initial stage of cement hydration, the capillary pores are all connected, and the cement matrix has a high permeability. With the increase of the degree of hydration, capillary pores decrease in volume and size and start to become disconnected; as a consequence, the permeability decreases as well. At a certain degree of hydration, the capillary pores are not connected any more, so that no connected path exists for the capillary transport; the result is a significant and sudden reduction in permeability. The value of the porosity at this hydration stage is called the "depercolation threshold". Important investigations about the influence of percolation on capillary transport in cementitious materials date back to the 1950s, when Powers et al. (1955, 1959) described the degree of hydration to achieve segmentation of the capillary pores in Portland cement pastes as a function of water-to-cement ratio (w/c) as reproduced in Table 1.

Table 1 Curing time (t) and degree of hydration (α) capable of segmenting the capillary pores in a Portland cement paste (Powers et al, 1959).

w/c	α (%)	t
0.40	50	3 days
0.45	60	7 days
0.50	70	14 days
0.60	92	6 months
0.70	100	1 year
>0.70	>100	Never

From the results of water permeability measurements, Powers et al (1959) concluded that the capillary pores in cement paste exhibit a percolation transition from connected to disconnected at about 20% porosity. This means that, regardless of the w/c ratio, when the capillary porosity in cement paste drops to 20%, no capillary transport is possible. The water permeability coefficient (defined in section 3.3.2) dramatically falls down to a certain value around 10^{-14} m/s when the capillary pores become depercolated. On the other side, whenever the measured permeability reached that value, depercolation of capillary pores had occurred.

However, the water permeability of cement paste reported by other authors shows significant variations as shown in Fig. 4 after Ye (2005). For example, parallel measurements of porosity and permeability by Mehta and Manmohan (1980) showed discrepancies with Powers' conclusion. Their experimental results indicated that the depercolation threshold of capillary porosity did not occur in cement pastes with w/c ratio above 0.30, even at ages up to 1 year. Results by Banthia and Mindess (1988) show similarities with Mehta and Manmohan's (1980) results for samples with w/c 0.35 at a curing age of 30 days. Detailed investigations have shown that the variations in water permeability are largely dependent on a series of factors; e.g. type of media (O_2, N_2, water or other liquid solutions) used in permeability tests (Hooton, 1988), sample preparation (Hillel, 1971), influence of curing conditions (sealed or saturated) and age of the sample and the pressure used in the permeability tests (Banthia and Mindess, 1988). The author of the present report may add the particle size distribution and the chemical composition of the cement as potential source of discrepancy. Thus, the existence of a percolation threshold of the capillary pores in cement paste appears to be both a relevant and a controversial subject.

The percolating network of pores for cement paste of w/c = 0.50 at 3 days is rather open, but as can be seen by the permeability coefficient as a function of time for cement paste at w/c = 0.70 in Table 2 (Powers et al, 1954) the permeability declines as time passes (or rather hydration proceeds). The minimum time to make the capillary pore network disconnected as a function of w/c is given in Table 3 (Powers et al, 1959).

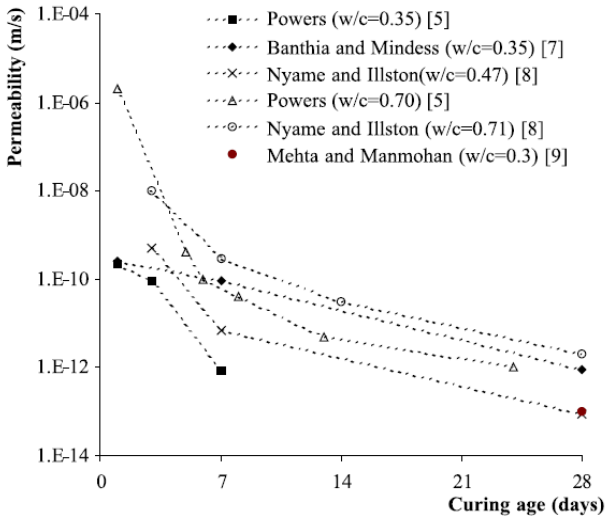

Fig. 4 Comparison of various permeability values reported by different authors (Ye, 2005)

Table 2 Reduction in permeability coefficients (according to d'Arcy) of hardened cement paste with w/c = 0.7 versus time of water storage (Powers et al, 1954).

Water curing time (days)	Permeability coefficient (10^{-12} m/s)
fresh paste	2,000,000
5	400
6	100
8	40
13	5
24	1
fully hydrated	0.6

Table 3 Minimum duration of water storage of hardened cement paste which is necessary to interrupt the initially continuous capillary pores by filling them with hydration products, as a function of w/c for a portland cement (Powers et al, 1959).

w/c	Minimum time of water storage
0.70	1 year
0.60	6 months
0.50	14 days
0.45	7 days
0.40	3 days

Fig. 5 shows permeability as a function of capillary porosity (Powers et al, 1954). A subsidiary diagram is included in Fig. 5 indicating the relationship between capillary porosity, w/c and degree of hydration by calculation in analogy to chapter 2.4 (Locher, 1973).

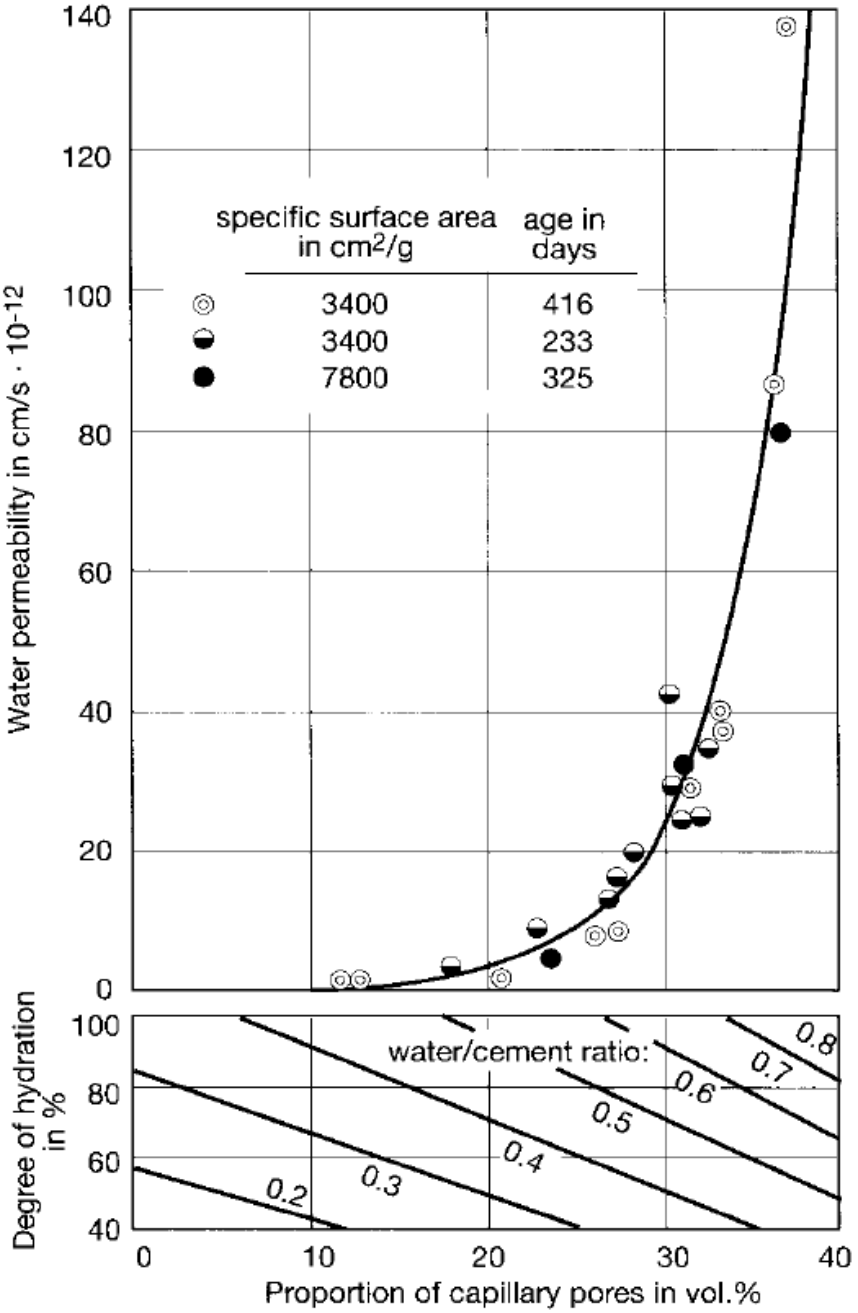

Fig. 5 Water permeability of hardened cement paste as a function of capillary porosity, w/c and the degree of cement hydration. Upper figure from Powers et al (1954) and lower figure from Locher (1973).

Many think that the cementitious binder is more permeable than the aggregate of the concrete. This is not necessarily true. Table 4 shows the permeability coefficient for a number of rocks and the corresponding w/c of a fully hydrated cement paste (Powers, 1958). Note that the transition zone between the matrix and in particular the coarser aggregate may be more permeable than the matrix. This is often referred to as a result of the "wall effect" where particles can not pack in an optimal way against the larger aggregate, as well as preferred growth of platelets of calcium hydroxide using the aggregate as substrate. The transition zone will be made less permeable with larger content of reactive fines like silica fume in the matrix.

Table 4 Permeability of some rocks compared to that of fully hydrated cement paste (Powers, 1958)

Rock type	Permeability coefficient (10^{-12} m/s)	w/c of fully hydrated cement paste with same permeability
dense igneous rock	0.0247	0.38
quartz-diorite	0.0824	0.42
marble 1	0.239	0.48
marble 2	5.77	0.66
granite 1	53.5	0.70
sandstone	123	0.71
granite 2	156	0.71

2.4 Total porosity of Portland cement paste

Portland cement paste is the mixture of Portland cement, water and any admixtures used. It is possible to estimate the porosity of hardened cement paste by assuming the degree of hydration (α) and the amount of chemical (23 %) and physical (17 %) bound water per mass of reacted cement. In addition, there will be contraction pores resulting from the chemical shrinkage as the reaction products have a smaller volume than the reactants (i.e. cement minerals and water). Contraction pores are empty ("vacuum") while non-reacted water constitutes water filled capillary pores. The water will always redistribute so the finest pores will be water filled on the expense of coarser ones due to capillary forces.

Before showing how to estimate total porosity, a more detailed description of chemical shrinkage leading to contraction pores is given. Knowing the density, ρ (g/ml), of reactants and products of a chemical reaction, it is possible from the molar weight, M (g/mol), of the involved compounds to calculate the volume change, ΔV (ml), per mass, m (g), reactant remembering the basic relations $n = m \cdot M$ (mol) and $\rho = m/V$.

The simplest example, the recrystallisation of hemihydrate to gypsum will per gram hemihydrate;

$$CaSO_4 \cdot \tfrac{1}{2}H_2O + 1\tfrac{1}{2}\,H_2O = CaSO_4 \cdot 2H_2O \qquad [2]$$

m = 1.00 g		0.19	1.19
M = 145.15 g/mol		18.02	172.17
n = 6.89 mmol		10.33	6.89
ρ = 2.74 g/ml		1.00	2.32
V = 0.365 ml		0.186	0.511

give a shrinkage of $\Delta V = 0.511-(0.365+0.186) = -0.040$ ml leading to empty contraction pores, whilst the volume of solid material is increased by $(0.511-0.365)\cdot 100\text{vol\%}/0.365 = 40\text{vol\%}$. The increase in solids volume (and subsequent reduction in total porosity), together with establishment of contact points between the hydrates, is why "plaster of Paris" (i.e. hemihydrate) hardens when blended with water.

In the proceeding chemical equations and formulas, cement chemist's short hand notation is used, where C = CaO, S = SiO_2, A = Al_2O_3, F = Fe_2O_3, H = H_2O, $\bar{C}$ = CO_2 and $\bar{C}$ = SO_3.

The approximate densities (g/ml) and molar weights (g/mol) required to do analogue calculations as for Eq. 2 are given in Table 5 for common substances in cement chemistry

Table 5 Densities and molar weights for some substances common in cement chemistry

Compound	Density (g/ml)	Molar weight (g/mol)
C_3S	3.15	228.32
C_2S	3.28	172.24
C_3A	3.03	270.20
C_4AF	3.73	485.97
$C\bar{S}H_2$	2.32	172.17
$C\bar{S}H_{0.5}$	2.74	145.15
$C_{4.7}S_{3.1}H_{5.9}$	2.49	552.3
CH	2.24	74.09
$C_6A\bar{S}_3H_{32}$	1.78	1,266.26
$C_4A\bar{S}H_{12}$	2.02	622.58
C_3AH_6	2.52	378.29
C_4AH_{13}	2.02	560.48
C_2AH_8	1.95	358.24

In this way one can also estimate the shrinkage of the initial Ettringite formation;

C_3A	+	3 $C\bar{S}H_2$	+	26 H	=	$C_6A\bar{S}_3H_{32}$ [3]
m = 1.00 g		1.91		1.73		4.64
M =270.20 g/mol		172.17		18.02		1255.26
n = 3.70 mmol		11.10		96.20		3.70
ρ = 3.03 g/ml		2.32		0.998		1.78
V = 0.330 ml		0.823		1.733		2.607

ΔV = 2.607 - (0.330+0.823+1.733) = -0.273 ml/g C_3A, while the chemical bound water is 1.73 g/g reacted C_3A, meaning that the chemical shrinkage is about 16 % of the chemical bound water. The increase in volume of solids are at the same time substantial; (2.607-(0.823+0.330))·100vol%/(0.823+0.330) = 126 vol%.

The chemical shrinkage of the alite reaction (alite, or impure C_3S, is the main mineral in Portland cement) can be estimated in a similar manner, but the magnitude is strongly dependent of the composition and density of the CSH-gel formed. Justnes and Kjellsen (2003) estimated the density of a 28 days CSH gel of composition $C_{4.7}S_{3.1}H_{5.9}$ to 2.49 g/ml, which leads to the chemical shrinkage of this balanced reaction;

C_3S	+	3.39 H	=	0.325 $C_{4.7}S_{3.1}H_{5.9}$	+	1.48 CH [4]
m = 1.00 g		0.267		0.787		0.480
M = 228.32 g/mol		18.02		552.3		74.09
n = 4.38 mmol		14.84		1.42		6.48
ρ = 3.15 g/ml		0.998		2.49		2.24
V = 0.317 ml		0.268		0.316		0.214

ΔV = (0.316+0.214) - (0.317+0.268) = -0.055 ml/g C_3S, while the chemical bound water is 0.27 g/g C_3S, meaning that the chemical shrinkage is about 8 % of the chemically bound water. Note that the chemical shrinkage of the C_3A reaction is much higher (≈ 5 times) than

the reaction of C_3S. On the other hand, the increase in volume of solids is smaller for C_3S compared to C_3A; ((0.316+0.214)-0.317)·100vol%/0.317 = 67 vol%.

The chemical reaction of the cement mineral C_4AF is more uncertain, but it is assumed to form products analogue to C_3A with some iron substitution for aluminium. However, the ferrite phase is often very slowly reacting and may remain unreacted for years. Since OPC often contain 10-15% C_4AF it is of vital importance for the permeability to get this phase to hydrate. Schwartz (1995) found that the addition of 1-3% tripotassium citrate was able to make the ferrite phase react within 6 h. Justnes et al (2008) also found considerable strength increase for mortars added citric acid, presumably due to activation of the ferrite phase.

The chemical shrinkage of Portland cement being a mixture of a number of minerals is in general considered to be about 0.06 ml/g cement (or about 25 % of the chemical bound water of 0.23 g/g cement reacted) according to Copeland and Hayes (1953).

The total porosity of a cement paste based on 1 g cement of density 3.15 g/ml and water-to-cement ratio (w/c) of 0.50 can then be calculated as follows assuming degree of hydration α = 0.80;

Chemical bound water = 0.23·0.80 = 0.184 g/g cement
Physically bound water = 0.17·0.80 = 0.136 g/g cement
Liquid water (ρ = 1.0 g/ml) = capillary porosity = 0.50-(0.184+0.136) = 0.18 ml/g cement
Contraction pores = 0.25·0.184 = 0.046 ml/g cement
Total porosity is then (0.18+0.046) ml·100 vol %/(1/3.15 + 0.5/1) ml = 27.6 vol %

In addition to the above calculated porosity comes entrained air, which is particularly important in concrete where the sand fraction seems to help stabilize air. The air content in a low viscosity cement paste is usually very low.

2.5 The influence of Ettringite on porosity and particle packing

As explained by Eq. 3, Ettringite is beneficial in reducing porosity of the hardened state since its formation transforms a lot of liquid water to solid hydrates, but at the same time this may be a part of the reason for reduced workability as pointed out by Justnes et al (2003). The elongated needle morphology of Ettringite may further influence rheology of cement matrix negatively. There is also a distinct possibility that needle shaped Ettringite shown in Fig. 6 may hamper initial packing of the cement grains in the fresh state and thereby lead to increased porosity and pore sizes in the hardened state.

Kerui et al (2002) attributed rapid loss of flow for fly ash containing cement paste to massive crystallization of needle shaped Ettringite when calcium lignosulphonate and sodium bicarbonate was added to the system.

Note that it is possible to alter the morphology of Ettringite from long needles to shorter ones or even mass-like by the use of different admixtures as for instance studied by Cody et al (2004).

It is also interesting to note that de Larrard and Sedran (1994) in their efforts to make ultra-high performance concrete by the use of a packing model, deliberately chose a low C_3A cement in order to minimize the water demand, but they did not mentioned the possibility of improved packing by less Ettringite formation in the fresh state.

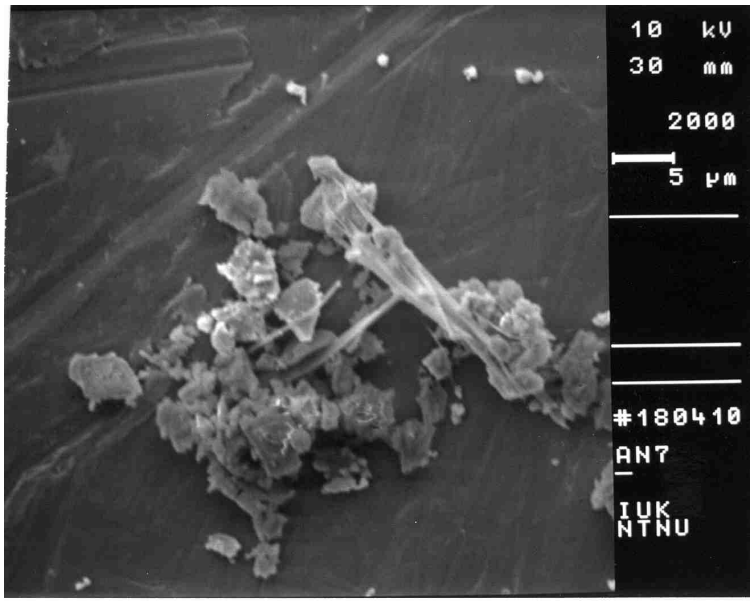

Fig. 6 SEM image of cement paste (20 min old) where water was replaced by excess ethanol and allowed to dry on a tape. Note that Ettringite needles are several times longer than the individual cement grains.

2.6 Total porosity of blended cement pastes

Modern cements are often a mixture of cement clinker and supplementary cementing materials (SCM) like blast furnace slag, fly ash, silica fume, lime stone filler etc. If these SCMs convert more liquid water per volume to hydrates than the cement they replace, and/or create hydration products of lower density than the cement, they may lead to lower total porosity.

Take for instance limestone filler that often is considered inert since it has so little calcium aluminate hydrate to react with in a Portland cement. The C_3A (usually 2-10% of cement mass) reaction in Eq. 3 leads initially to Ettringite ($C_6A\bar{S}_3H_{32}$), but there is normally not enough gypsum ($C\bar{S}H_2$) to balance all C_3A, so when the C_3A continue to hydrate it will transform Ettringite to so called monosulphate ($C_4A\bar{S}H_{12}$);

$$2\ C_3A + C_6A\bar{S}_3H_{32} + 4\ H = 3\ C_4A\bar{S}H_{12} \qquad [5]$$

However, over time the monosulphate is unstable in presence of limestone and will form calcium carboaluminate hydrate ($C_4A\textcircled{c}H_{11}$) and the released sulphate may then react with monosulphate to form Ettringite again, which is stable in presence of limestone (Matschei et al., 2007a, b and c);

$2\ C\bar{C}$	+	$3\ C_4A\bar{S}H_{12}$	+	$18\ H = 2\ C_4A\bar{C}H_{11}$	+ $C_6A\bar{S}_3H_{32}$
m = 1.00 g		9.33		1.62	5.68	6.27
M =100.09 g/mol		622.58		18.02	568.50	1255.26
n = 9.99 mmol		14.99		89.91	9.99	5.00
ρ = 2.67 g/ml		2.02		0.998	2.17	1.78
V = 0.375 ml		4.619		1.623	2.618	3.522

[6]

According to Eq. 6, 100 g (= 1 mole) of calcium carbonate ($C\bar{C}$) will bind 18/2 = 9 mole (162 g) of extra liquid water, while cement binds 23 g water per 100 g reacted cement as

comparison. Using density 2.17 g/ml of calcium carboaluminate hydrate ($C_4A\bar{C}H_{11}$) from Matschei et al (2007b), the total increase in volume of solids can be calculated to ((2.618+3.522)-(4.619+0.375)·100vol%/(4.619+0.375) = 23 vol%.

If there was even more C_3A in the cement, another stable phase after the hydration would have been calcium aluminate hexahydrate (C_3AH_6) that also can react with limestone to form calcium carboaluminate hydrate;

$C\bar{C}$ +	C_3AH_6 +	5 H	=	$C_4A\bar{C}H_{11}$	[7]
m = 1.00 g	3.78	0.90		5.68	
M =100.09 g/mol	378.29	18.02		568.50	
n = 9.99 mmol	9.99	49.95		9.99	
ρ = 2.67 g/ml	2.52	0.998		2.17	
V = 0.375 ml	1.500	0.902		2.618	

According to Eq. 7, 100 g calcium carbonate (1 mol) would then bind 90 g (5 mol) extra water. The total increase in volume of solids according to Eq. 7 is then (2.618-(0.375+1.500))·100vol%/(0.375+1.500) = 40 vol%. So the replacement of cement with limestone would have been very efficient in lowering total porosity had there only been more calcium aluminate hydrate in the system. Increasing the C_3A is not a viable option, due to more sulphate required to control setting and thereby more initial Ettringite formation hampering packing. Calcium aluminate hydrates may, on the other hand, be produced after setting by aluminate containing supplementary cementing materials (e.g. slag, fly ash, metakaolin).

Usually, more limestone is added to cement than what can react with the aluminates present in the cement, even when one take into account hydration of the ferrite phase (C_4AF). A portland cement containing for instance 5% Al_2O_3 could only in theory consume 5%·100/102 • 5% calcium carbonate (using the molar ratio 1 from Eq. 7 and the molar weights 100 and 102 g/mol for $CaCO_3$ and Al_2O_3, respectively) if all the aluminate was converted to calcium carboaluminate hydrate, which is not the case since a fraction of it will end up as stable Ettringite (see Eq. 6). Lothenbach et al (2008) recently used thermodynamic modelling to calculate the phase assembly and porosity of cement with limestone and found good correlations with measured strength evolution.

Making cement with unusual high C_3A content would eventually make it difficult to control in terms of setting. Another possibility is to combine limestone with SCMs that will form calcium aluminate hydrates in their reaction as already pointed out. De Weerdt and Justnes (2008) tested this hypothesis by blending siliceous fly ash with lime and alkaline water (to simulate the situation in a portland cement) and with/without limestone. Siliceous fly ash consisting of a glassy aluminosilicate (AS) phase forms a mixture of calcium silicate hydrate (CSH) gel, Strätlingite (C_2ASH_8) and calcium aluminate hydrates (e.g. C_3AH_6) in reaction with calcium hydroxide (CH). The following pozzolanic reaction is unbalanced since there are too many unknowns;

$$CH + AS + H \rightarrow CSH + C_2ASH_8 + C_3AH_6 \quad [8]$$

De Weerdt and Justnes (2008) found indeed that the calcium aluminate hexahydrate (C_3AH_6) was formed between 5 and 38°C and that calcium carboaluminate hydrate was present when calcium carbonate was included in the mix. They also proved that the total mass loss (105-1000°C) increased with increasing time, meaning that the pozzolanic reaction of the fly ash binds more water than what is inherent in the calcium hydroxide (i.e. one mol H_2O per mol $Ca(OH)_2$ taking part in the pozzolanic reaction). However, it is uncertain whether the fly ash would bind more water per volume unit than the replaced cement.

Tangpagasit et al (2005) compared the strength of mortars with fly ash with that of mortar with inert filler with same particle size distribution of fly ash in order to distinguish the effect of particle packing to that of the pozzolanic reaction. They found that effect of particle packing was much greater than the pozzolanic effect at early ages and also at later ages for the coarsest fly ash.

Pozzolans like calcined clays (e.g. metakaoline) will give essentially the same hydration products as sketched in reaction 8.

The chemically simplest SCM is silica fume (SF) since it usually consist of > 90 % amorphous SiO_2 (S) spheres with average individual diameter of 0.15μm, although these may be agglomerated. It is a pozzolan, meaning that it reacts with calcium hydroxide (CH) forming additional binding CSH-gel as shown by the overall reaction

$$CH + S = CSH \qquad [9]$$

However, this reaction would take months to bring about strength if it was not for the catalytic action of alkali hydroxides in the pore water of hardened cement bringing it to days as shown in the reaction loop (Justnes, 2007);

$$\begin{array}{l} S\,(s) + (N,K)H\,(aq) \rightarrow (N,K)SH\,(aq) \\ \qquad\quad \uparrow \qquad + \\ CSH\,(s) + (N,K)H\,(aq) \leftarrow CH\,(aq \text{ or } s) \end{array} \qquad [10]$$

using cement chemist's short hand notation; C = CaO, S = SiO_2, N = Na_2O, K = K_2O and H = H_2O. Silica fume does not seem to bind more water chemically than what is inherent in CH, but due to the large surface of CSH, more may be bound physically.

Blast furnace slag is not a pozzolan, but has self-cementing properties when activated by sulphates or alkali hydroxides. Blast furnace slag has a typical composition of 47 % CaO+MgO, 35 % SiO_2 and 12 % Al_2O_3. When activated with gypsum together with cement, the hydration products are generally the same as for ordinary Portland cement (OPC); CSH-gel, Ettringite and monosulphate (Schmolczyk, 1965, and Uchikawa, 1986). The formation of Strätlingite (C_2ASH_8) is only to be expected if alkali hydroxide is added to the slag cement (Richartz, 1966) or if the blast furnace slag is activated with alkali hydroxide (Regourd, 1980, and Forss, 1983).

3 METHODS FOR MEASURING OPTIMUM PARTICLE PACKING

3.1 In the fresh, wet state

3.1.1 Introduction

The loose bulk density of dry particles can be determined according to EN 1097-3. The method can be extended to determine the maximum packing density at a certain compaction level, by applying external loads such as vibration or top-weight. However, cement dry packing is of little interest since it is going to be mixed with water and the situation will be quite different due to dissolution of salts, different surface charges, Ettringite growth on the particle surface, etc. To determine the maximum packing density of wet particles no single method is generally accepted and therefore different countries use their own test methods to determine packing density and/or water demand of fine particles.

3.1.2 French water demand test (de Larrard, 1999)

This method aims at finding the minimum water dosages to produce a thick paste. A slightly lower amount of water should give a humid powder. Since the water demand measurement is influenced by the type and amount of superplasticizer, it should be dosed as a percentage of the powder mass. A mass of 350 gram of powder is mixed with water according to the procedure: The amount of water at minimum water demand is estimated (Eq. 11) and mixed with the superplasticizer. First the water (including SP) is added to the mixing bowl, then the powder. The paste is mixed for 1 minute at low speed, then rested/ scraped and subsequently mixed for one minute at high speed. During the mixing at high speed an extra amount of water is added using a pipette to adjust the workability of the paste. The test is repeated with a slightly lower amount of water than in the first test until it becomes a thick powder. The packing density of the powder is calculated by Eq. 11, as average of two tests, in which the amount of water in the pipette was lower than 5 grams.

$$PD = \frac{1{,}000}{1{,}000 + \rho \dfrac{m_w}{m_p}} \qquad [11]$$

PD = packing density
m_w = mass of the water
m_p = mass of the powder
ρ = density of the powder in kg/m^3

The difficulty of the method is recognizing the transition from a humid powder to a thick homogeneous paste, especially when the humid powder forms a sticky non-homogeneous ‘paste’.

3.1.3 German water demand test (Puntke, 2002)

The method is based on the idea that a fine, low-cohesion particle packing without a load, then and only then can be compacted to a specific value for the powder, when the water content is sufficient to fill all the voids in that packing. With humid, but not yet saturated packed particles, the surface tension (capillary forces) will block the water from surrounding the particles. At the saturation point the capillary forces will disappear and the particles can easily be packed to the characteristic highest packing density. The compaction energy is not important, but the compactability. The transition from ‘not yet compactable’ to ‘compactable’ can occur by adding just 0.1 grams of water to a sample containing 100 gram of powder. An excess amount of water will also lead to possible compaction, but it will result in a lower packing density or possible bleeding. For this reason it is very important to approach the saturation point by carefully adding water according to the following

procedure: Place 50 grams of powder in a plastic or metal container with a flat bottom. Water is added slowly by making use of a siphon/pipette while the humid powder is mixed with a steel blade or rod. The saturation point is reached when after repeatedly tapping against the container the powder surface levels off and starts to shine. The test should be repeated at least two times with a slightly lower amount of water. The final water demand is calculated according to Eq. 11 from the smallest amount of water of three tests.

A disadvantage of the test is that the method can only confidently be used when the existence of air voids in the 'saturated paste' can be ruled out.

3.1.4 Japanese water demand test (Okamura and Ozawa, 1995)

This method is based on the idea that the water demand of a mixture can be determined indirectly from a linear relationship between the relative flow area R_p in Eq. 12 and the water by powder ratio by volume V_w/V_p .

$$R_p = \frac{D^2 - D_0^2}{D_0^2} \qquad [12]$$

D = the average spread diameter in a slump flow test

D_0 = the base diameter of the cone in a slump flow test.

When R_p would be zero, $D = D_0$ and no flow is initiated. This state is considered to be achieved when the amount of water in the paste is just sufficient to adsorb on the particle surfaces and fill all the voids in the particle system (saturation point). This saturation point which corresponds to a certain V_w/V_p is called the retained water ratio β_p (or water demand). Since it is not possible to perform a slump flow test on mixtures with a water powder ratio close to the saturation point a number of mixtures with higher water powder ratios are tested and β_p is calculated from the linear relation between V_w/V_p and R_p as the interception point when R_p is zero.

For this method, measurements were performed according to the following procedure: A paste, with a known composition, is mixed in a three-litre Hobart mixer. First, the dry powders are mixed for ten seconds after which the water and superplasticizer are added. The paste is mixed for 1 minute at low speed, then rested / scraped for one minute and subsequently mixed for another minute at low speed. The slump flow was determined by a mini cone test (upper/lower diameter 20/37 mm and height 57 mm) on a flow table (Tonindustrie) with a 300 mm diameter glass plate. The slump flow is taken as the average spread diameter, calculated in four directions.

3.1.5 Water demand by mixing energy (Marquardt, 2001)

When water is added to a powder it condenses on the particles to form capillary bridges (pendular bonds) localized at the particle contacts. In this way, agglomerates of particles are formed. The strength of the pendular bond increases with the liquid-vapour surface energy and depends inversely on the square of the particle diameter. At less than total saturation, the strength of the agglomerates increases with the amount of liquid and the surface energy of the liquid. The absence of internal liquid-vapour surfaces at 100 % saturation causes the strength to suddenly decrease at this point (Puntke, 2002).

The method described by Marquardt (2001) is based on the idea that the differences in internal pendular bond strength can be measured by measuring the mixing energy according to the following procedure: A powder volume of about 200 cm^3 is mixed in a mortar mixer (EN 196, Part 1), with a constant water supply of 1.5 ml/s during the entire mixing time, at a mixing speed of 140 rpm. During mixing, the voltage, electricity consumption and the phase shift between the voltage and the electricity consumption of the mixer are registered to

determine power use. The water demand of the mix is recorded as the water to powder ratio at which maximum power use is measured and Eq. 11 can be used to calculate the packing density.

3.1.6 Proctor test (EN 13286-2)

The proctor test is normally used to determine maximum mixture density of unbound and hydraulically bound mixtures used in road construction and civil engineering work. However, it can also be used on fine powders. In that case a powder is mixed thoroughly with a certain amount of water. The moist mixture is placed in a mould (diameter 100 mm, height 120 mm) in three layers, such that after compaction the sample is higher than the mould body. After placing each layer it is compacted by applying 25 blows of a 2.5 kg rammer dropped from a height of 305 mm above the mixture in such way that the blows are uniformly distributed over the surface of the sample. The extension of the mould is removed and the surface of the compacted mixture is carefully levelled off. After determining the mass of the sample (moist mixture) by weighing, the water content w is determined by drying according to EN 1097-5. The compacted dry density of the mixture is calculated for each compacted sample by Eq, 13.

$$\rho_d = \frac{100\rho}{100 + w} \qquad [13]$$

ρ_d = dry density [g/cm^3]
ρ = bulk density of the sample after proctor compaction [g/cm^3]
w = water content of the mixture [%]

The dry densities obtained from at least five determinations with different water contents are plotted against the corresponding water contents. A curve of best fit is drawn to the plotted points to identify the position of the maximum on this curve. The dry density at the maximum of the curve is considered to correspond to the maximum achievable packing density of the moist mixture.

Unfortunately, because of the necessary drying of the powder after testing to determine the water content, this method is not suitable do determine the packing density of cement very accurately.

3.1.7 Centrifugal consolidation (Miller et al, 1996)

The particle packing density of a powder can be determined by centrifugal consolidation according to the following procedure: A paste, with a known composition, is mixed in a three-litre Hobart mixer. First, the dry powders are mixed for ten seconds after which the water and superplasticizer are added. The paste is mixed for 1 minute at low speed, then rested/ scraped for one minute and subsequently mixed for another minute at low speed. The paste is poured into 90 mm long test-tubes with an internal diameter of 22 mm. By determining the mass of the paste in the test-tube, the amounts of powder and water in the test-tube at the beginning of the test are known. The test-tube is then centrifuged for ten minutes at 4,000 rounds per minute in a Dumee Jouan E82N Centrifuge with an internal diameter of ± 300 mm. By centrifuging the test-tubes, the particles in the paste are compacted and less amount of water is necessary to fill the voids in the compacted particle matrix. Therefore, the total sample will possess an excess amount of water, which will occur as a water layer on top of the (compacted) paste. This water layer can be removed with a pipette, after centrifuging. By determining the amount of removed water, the amount of water and particles in the compacted sample are known and thus the packing density of the powder can be calculated using Eq. 11.

3.1.8 Viscosity of suspensions

3.1.8.1 Theory

Einstein derived in 1906 a relationship between the viscosity of a suspension and the solid fraction for diluted suspensions of spherical particles (10% and less solid concentration). This relationship is:

$$\frac{\eta}{\eta_c} = \left(1 + 2.5 \cdot \varphi\right). \qquad [14]$$

where η is the viscosity of the suspension, η_c is the apparent viscosity of the continuous phase and φ is the solid concentration (volume fraction). In this relationship he assumed that there is no interaction between the particles, but as soon as the concentration increases and the particles start to interact the situation becomes more complicated.

Krieger and Dougherty (1959) found a relationship between the viscosity and the solid concentration for well dispersed suspensions with a higher solid concentration. The relation is the following:

$$\frac{\eta}{\eta_c} = \left(1 - \frac{\varphi}{\varphi_m}\right)^{-[\eta]\varphi_m} \qquad [15]$$

where η is the apparent suspension viscosity, η_c is the continuous (liquid) phase viscosity (η_c = 0.001Pa.s for pure water at 20°C), φ is the solid concentration (volume fraction), φ_m is the maximum concentration possible for the particular system and $[\eta]$ is the intrinsic viscosity of the suspension given by

$$[\eta] = \lim_{\varphi \to 0} \frac{\frac{\eta}{\eta_c} - 1}{\varphi} \cong 5 \qquad [16]$$

All independent variables; concentration, particle size distribution and particle shape, relate to the density at which particles are packed in suspension. Both φ_m and $[\eta]$ depend on shear stress, τ. For spherical particles φ_m is 0.63 at $\tau \to 0$ and 0.71 at $\tau \to \infty$. There is no theoretical basis of calculating φ_m for polydisperse particles, but it can be obtained empirically from viscosity of suspensions at various volume fractions as was done for cement paste by Justnes and Vikan (2005). Mansoutre et al (1999) also found that C_3S paste at various concentrations fit very well to the Krieger-Dougherty equation given in Eq. 15.

The Krieger-Dougherty equation includes effects of particle size distribution and particle shape (Barnes et al, 1989), but not effects of particle sizes with same relative size distribution. Thus, suspensions of monosized particles will have the same φ_m and the same viscosity even if their particle size is different. The parameter φ_m increases with increasing polydispersity. The *polydispersity* of a cement powder can be investigated from its particle size distribution (PSD) using the Rosin-Rammler (RR) distribution function also called Rosin-Rammler-Sperling-Bennet (RRSB) distribution function (Locher, 2006):

$$R(x) = e^{\left(\frac{x}{x'}\right)^n} \qquad \text{or} \qquad \ln\{R(x)\} = \left(\frac{x}{x'}\right)^n \qquad [17]$$

where R(x) is the weight fraction of particles larger than x, x is the particle diameter in μm, x' is the position parameter, also called characteristic diameter, and n is the uniformity index. In a typical RRSB granulometric diagram, ln{ln{1/R(x)}} is used as the ordinate and ln{x} as the abscissa. Then the PSD results approximately in a straight line. The characteristic diameter x' is a measure of the fineness of the RRSB distribution and can be found from the intercept of the ordinate -n·ln(x') knowing n as the slope of the RRSB straight line. The value of n is a measure of the width of the distribution or in other words the *polydispersity*. The larger the value of n, the narrower is the particle size distribution.

Wang et al (1999) analyzed theoretically the influence of the particle size distribution according to the RR function on the property of cement. They concluded that: (1) A wider particle size distribution is advantageous for increasing the packing density of the system and decreasing the water demand. The less the uniformity index (n), the higher is the packing density and the lower the water demand is. (2) Narrower particle size distribution is advantageous to raise the hydration rate. The larger the uniformity index, the higher is the hydration rate (3). Under the condition of the same water-cement ratio, narrow particle size distribution is advantageous to reduce the porosity of cement paste. Under the condition of the same hydration degree, wide particle size distribution is advantageous to reduce the porosity of cement paste. In the more practical sense, there should be an optimum particle size distribution. It occurs when *n* equals 1.

3.1.8.2 Measuring improved packing by suspension viscosity

The apparent viscosity of cement suspensions with a range of relevant w/c-ratios (i.e. solids content) can be fitted very well to the Krieger-Dougherty equation (Eq. 15) as demonstrated by Justnes and Vikan (2005) and reproduced in Table 6 and Fig. 7.

De Weerdt (2008) carried out similar experiments on suspensions of untreated fly ash (FA U), finely ground fly ash (FA FM), finely ground limestone (L FM) as well as 80% FA U and 20% L FM combination. The fitting of the Krieger-Dougherty equation to the apparent viscosity of the slurries is reproduced in Fig. 8 and the resulting parameters listed in Table 7. The parameters of fitting the RRSB function in Eq. 17 to the PSDs (plotted in Fig. 9) of the same powders are given in Table 8.

Table 6 Measured and calculated apparent viscosities (η_{meas} and η_{calc}) in mPa·s at different shear rates ($\dot{\gamma}$) for CEM I 42,5 RR cement slurry with 1.32% lignosulphonate as a function of solids fraction (φ) together with the fitting parameters in Eq. 15 (φ_{max} and [η]) and the regression factor (R^2).

$\dot{\gamma}$ (s^{-1})		9.79		2.75	
φ	w/c	η_{meas}	η_{calc}	η_{meas}	η_{calc}
0.36	0.564	61	49	122	87
0.38	0.518	66	78	129	149
0.40	0.476	147	137	312	284
0.42	0.438	340	280	830	649
0.44	0.404	723	750	1980	2029
0.46	0.373	3750	3726	13100	12883
φ_m =			0.484		0.484
[η] =			5.397		6.263
R^2 =			0.9995		0.9997

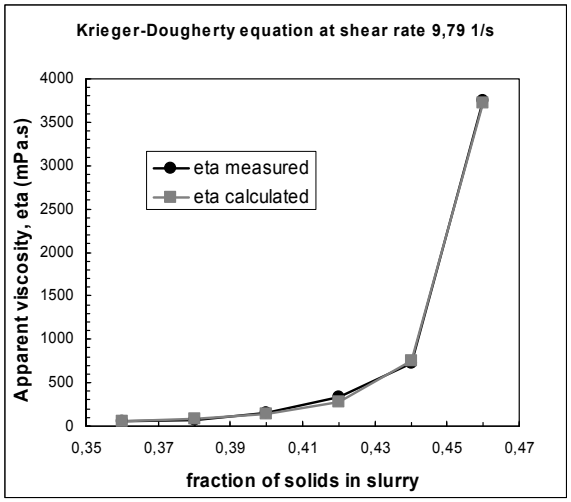

Fig. 7 Measured and calculated (Eq. 15) apparent viscosity (η) for cement slurries as a function of volume fraction of solids (φ) at a shear rate ($\dot{\gamma}$) of 9.79 s^{-1} for a CEM I 42,5 RR cement slurry dispersed with 1.32% lignosulphonate in a high shear mixer.

Table 7: Parameters obtained by fitting measurements to the Krieger-Dougherty equation (De Weerdt, 2008).

	shear rate					
	10 s^{-1}			30 s^{-1}		
	φ_m	[η]	R^2	φ_m	[η]	R^2
FA U	0.586±0.003	5.0±0.1	0.9980	0.592±0.003	5.0±0.1	0.9968
FA FM	0.570±0.002	7.9±0.1	0.9996	0.569±0.002	7.3±0.1	0.9997
L FM	0.698±0.004	8.4±0.1	0.9997	0.666±0.003	7.0±0.1	0.9997
20% L FM/80% FA U	0.607±0.003	5.4±0.1	0.9988	0.615±0.003	5.3±0.1	0.9983

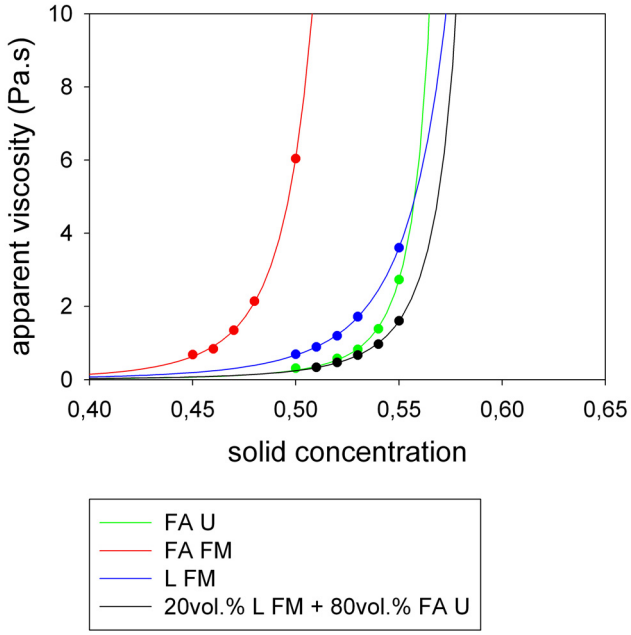

Fig. 8 Apparent viscosity as function of the solid concentration in slurries of the solids shown in the legend box at a shear rate of 30 s^{-1}. The measurements are indicated by dots, while the full lines represent the curves fitted to the Krieger-Dougherty equation (De Weerdt, 2008).

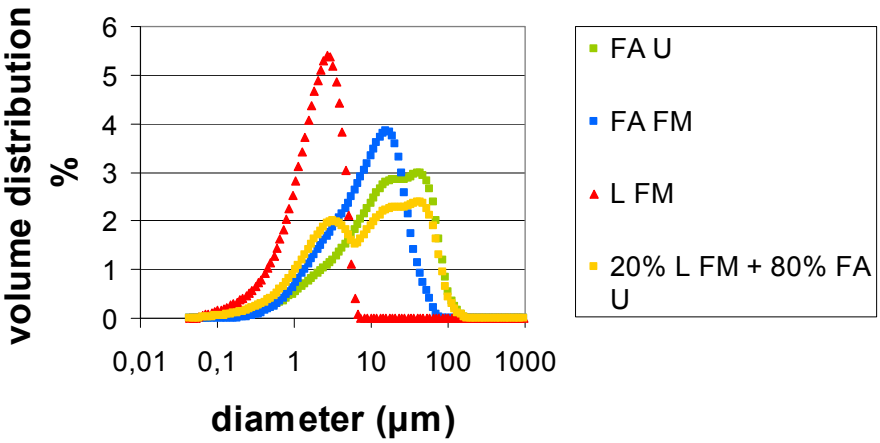

Fig. 9 Particle size distribution of the different dry powders used by De Weerdt (2008).

Table 8: RRSB parameters and regression coefficient (R^2) from the fitting to the PSD (De Weerdt, 2008).

	x' (µm)	n	R^2
FA U	20	1.2	0.98
FA FM	12	1.7	0.91
L FM	4	1.9	0.92
20% L FM/80% FA U	6	1.1	0.96

The larger the uniformity index n in Table 8, the narrower the PSD. This means that the order of increasing polydispersity of the solids is: L FM < FA FM < FA U < 20% L FM/80% FA U, which in theory should follow the order of φ_m from Table 7. That is OK for the fly ashes, but the limestone has much higher φ_m than expected from the n value. It is possible that the relation only holds for powders of the same nature.

The present conclusion is that instead of relating optimal packing of multiple powders to φ_m, it might be better for a diagram as in Fig. 8 to choose a relevant apparent viscosity for the application of the slurry and from the crossing of the curves see which mix that gives the highest volume of solids (preferably within the measured range). That should be the suspension with optimal particle packing.

This approach would for an apparent viscosity of about 2 Pa·s give the order of highest volume of solids FA FM < L FM < FA U < 20% L FM/80% FA U (with only the two lowest, close ones being shifted compared to n in Table 7), while the largest φ_m gives the order FA FM < FA U < 20% L FM/80% FA U < L FM.

Note that the Krieger-Dougherty approach has a drawback for hydrating particles like cement or water absorbing particles (may be the case for FA FM) since one are plotting apparent viscosity versus ***nominal*** solid fractions while one are measuring on ***effective*** volume fractions that should shift the curves in Fig. 8 to the right if it was corrected for. It should be possible to correct for cement with hydrate water by liquid replacement of ethanol, followed by thermogravimetry to measure amount of bound water at the relevant time of viscosity measurements (should be same for all solid volumes). However, it may potentially be more difficult to correct for porous inert particles simply absorbing water that from a viscosity standpoint will be experienced as solid. Justnes et al (2003) pointed out for cement that there is a double effect by removing liquid water (continuous phase) **and** transferring it

to a solid phase, since both alone would have lead to higher φ as shown in Eq. 18 and given an effective w/c according to Eq. 19.

$$(\varphi)_{hydr} = \frac{\left\{\left(\frac{(1-\alpha)\cdot c}{\rho_c}\right)+\left(\frac{(1+0.40)\cdot c\cdot\alpha}{\rho_{hydr}}\right)\right\}}{\left\{\left(\frac{(1-\alpha)\cdot c}{\rho_c}\right)+\left(\frac{(1+0.40)\cdot c\cdot\alpha}{\rho_{hydr}}\right)+\left(\frac{(1-0.40\cdot\alpha)\cdot w}{\rho_w}\right)\right\}} \quad [18]$$

$$\left(\frac{w}{c}\right)_{hydr} = \frac{(1-0.40\cdot\alpha)\cdot w}{(1+0.40\cdot\alpha)\cdot c} \quad [19]$$

where ρ_c, ρ_{hydr} and ρ_w are the densities of cement, hydrate and water, respectively, c is mass of cement, w is mass of water and α is degree of hydration.
According to Eq. 18, w/c = 0.40 and a change in α from 0.00 to 0.05 (5%) means a change in apparent viscosity, η, from 42.4 to 52.3 mPa·s according to the Krieger-Dougherty equation (Eq. 15) or a relative viscosity change of $\Delta\eta/\eta$ = 23%.

The sensitivity of rheological change to surface hydration in the fresh state increases at lower w/c. For instance, w/c = 0.30 and a change in α from 0.00 to 0.05 means a change in apparent viscosity, η, from 171 to 239 mPa·s, or a relative viscosity change of $\Delta\eta/\eta$ = 40%.

3.2 Shortly after setting

3.2.1 Porosimetry

Another potential method of finding optimum particle packing is to fill the fresh matrix in small glass vials with a plastic lid and place them in the curing temperature as required. These vials can then be quenched in liquid nitrogen (-196°C) every half hour (or even more often). The glass is broken and removed and the frozen sample allowed thawing in excess ethanol. If it has not set, the sample will fall apart to a powder. If it has set, it will retain its shape. This weak material after setting can be subjected to mercury intrusion porosimetry (MIP) for determination of pore size distribution.

This procedure is exemplified in Fig. 10 for cement pastes designed for oil-well cementing at 150°C immediately after setting when very little has reacted (Justnes 2007). The figure shows that silica fume (SF) alone reduced the average pore size openings from about 250 nm to 25 nm.

The effect of grinding on particle packing, or rather pore size openings, was studied with the same technique for a 50/50 mix of OPC/quartz blended (denoted Q) or ground by the energy modified cement (EMC) technique (denoted EQ), as well as for a 50/50 OPC/fly ash mix denoted FA and EFA, respectively. The data are taken from Justnes et al (2005) and replotted in Fig. 11.

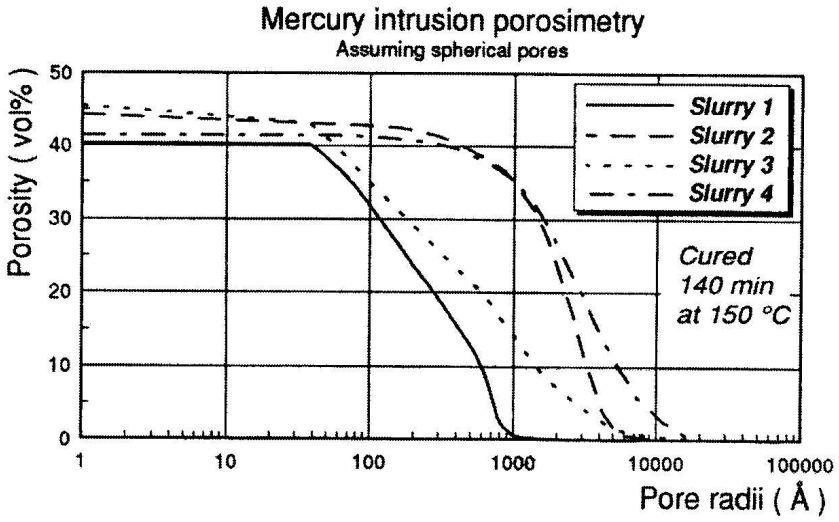

Fig. 10 Pore size distribution of oil well cement slurries immediately after set at 150°C: 1) complete composition, 2) lacking SF, 3) lacking weight material (i.e. fine Mn_3O_4) and 4) lacking both SF and weight material (Justnes, 2007).

It appears like the fineness of the particles is determining the size of the pore openings if they are sufficiently abundant to disperse coarser ones, which is obvious from the discussion of basic particle packing in Chapter 2.1. Thus, making smallest possible reacting particles would give the ultimate low pore opening size and thereby the lowest porosity if they are added at a relatively high dosage. The challenge is then to make them in the most economical way (grinding is expensive and limited to a certain size) and at the same time not let them hamper workability by being too reactive in the fresh state. Thus, the fine tail of PSD of for instance of a ternary cement should consist of particles of slow reactivity like nano-sized calcium carbonate made from precipitation reactions or perhaps fine recycled glass powder.

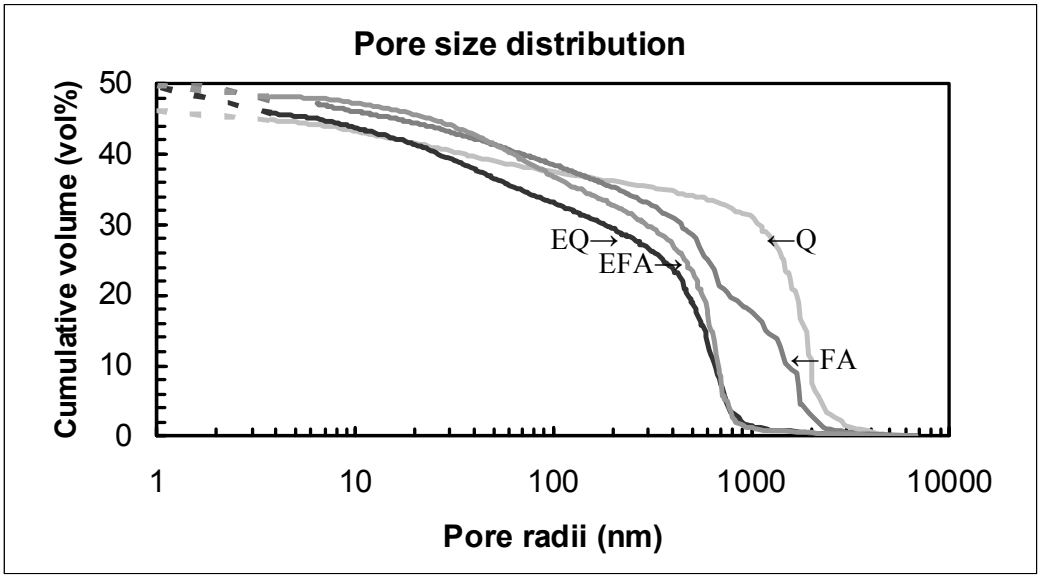

Fig. 11 Pore size distribution of EQ (w/s = 0.40) and EFA (w/s = 0.50) pastes cured for 6 h at 20°C and Q (w/s = 0.40) and FA (w/s = 0.50) pastes cured for 12 h at 20°C. Solid line from mercury intrusion porosimetry and dashes line residual porosity from helium pychnometry (Justnes et al, 2005).

3.2.2 Synchrotron X-ray micro tomography

With the development of synchrotron radiation sources a novel method of studying total porosity and connected pores has been developed (Gallucci et al, 2007), called synchrotron X-ray micro tomography. The resolution of the method is comparable to what is obtained by SEM as reproduced in Fig. 12 for a slice of a glass tube filled with cement paste of w/c = 0.50. The 2D images obtained at different heights of the paste in the glass tubes can then be coupled together in 3D and pores sorted out according to their dark grey-tone values. Further computation can then differentiate between total porosity and pores being interconnected to form a percolating network as shown in Fig. 13.

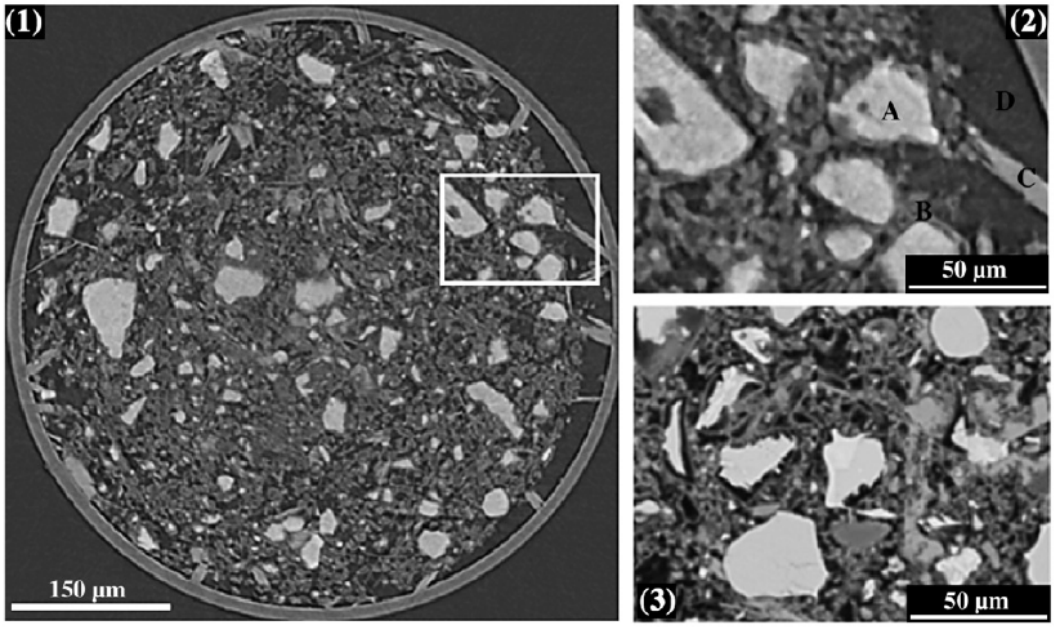

Fig. 12 Results from synchrotron X-ray microtomography showing (1) Reconstructed slice of a 1 day old OPC paste of w/c = 0.50. (2) Zoomed part of rectangle in (1). (3) Comparison with similar specimen in SEM. Mark A = unreacted cement grains, B = inner CSH, C = calcium hydroxide and D = unfilled spaces (air or water filled porosity). The figure is taken from Gallucci et al (2007).

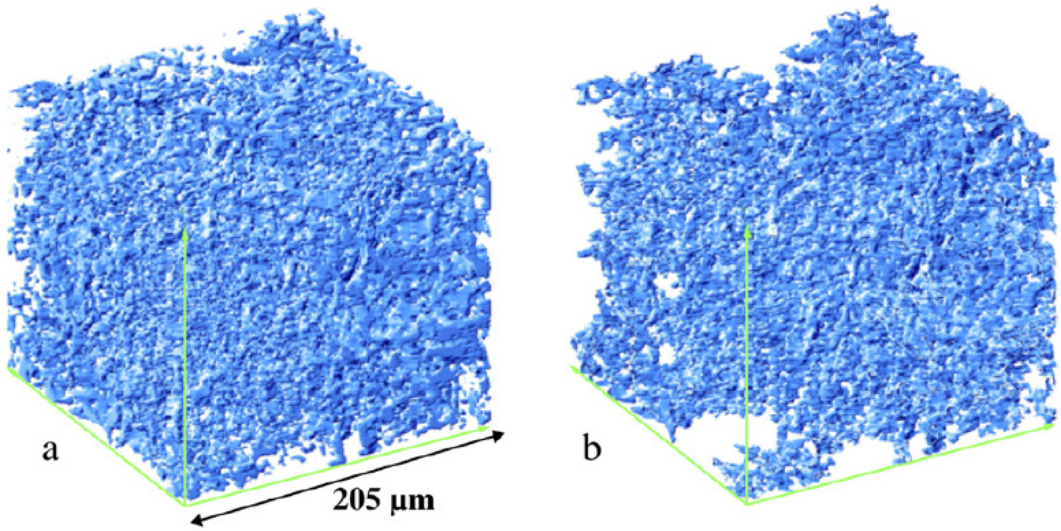

Fig. 13 Total porosity (a) and percolating pore network (b) of a 3 days old OPC paste of w/c = 0.50 (Gallucci et al, 2007).

3.3 On well hydrated specimen

3.3.1 Diffusion

Diffusion is the transport of ions or molecules caused by gradients in concentration or partial pressure, and the molecular movement when the overall pressure gradient is zero. Generally, the only known quantities during diffusion measurements on hardened cement paste, mortar or concrete samples are the outer surface area of the sample being exposed to the solution or gas mix and the thickness of the sample. The total of the pore cross-sections and the total of the pore lengths in the direction of diffusion, which actually govern the diffusion, remain unknown. It is also to be expected that other types of diffusion, e.g. molecular and surface diffusion, will be superimposed on the volume diffusion. An *effective* (also called apparent) diffusion coefficient of the hardened cement paste, mortar or concrete sample is therefore generally used.

Diffusion **through** (steady state flow) porous media, e.g. concrete, can be modelled by a linear diffusion equation, Fick's 1st law, in the following form for one dimension;

$$J = \frac{\delta s}{\delta t} = -D \cdot \frac{\delta C}{\delta t} \qquad [20]$$

$$J = \frac{\delta s}{\delta t} = -\frac{D_{eff} \cdot A \cdot \Delta C}{L} \qquad [21]$$

Where J, or $\delta s/\delta t$, is the quantity of substance in question diffused per time interval [mol/s or g/s] through the porous media of area A [m^2] and thickness L [m], ΔC is the concentration difference of the substance [mol/m^3 or g/m^3] across the material thickness L and D_{eff} is the *effective* diffusion coefficient [m^2/s]. J is often called the flux of substance diffusing.

For pure diffusion, one can use a set-up as given for chloride diffusion in NT Build 355 and reproduced in Fig. 14, without applying an electrical field, or one can get faster results by applying an electrical field, but it is then *electromigration* rather than *diffusion*. The formulas for diffusion coefficients from pure steady state diffusion and electromigration are given in Eqs 22 and 23, respectively. It has been shown that the relative difference between chloride diffusion coefficients of samples from electromigration experiments just as well can be obtained even faster by measuring electrical conductivity. This statement also holds for the high voltage method of ASTM C 1202 – 94.

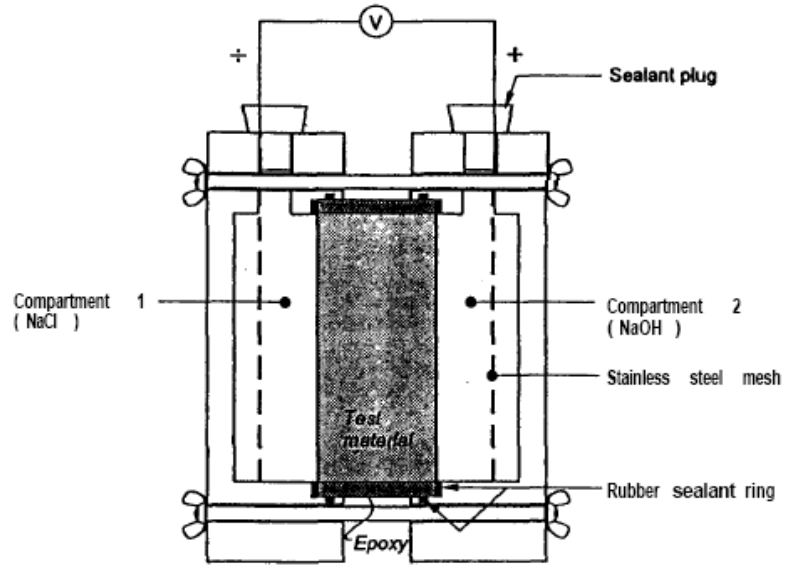

Fig. 14 The electromigration cell of NT Build 355.

$$D_{eff} = \frac{-J \cdot L}{A \cdot \Delta C} \quad [22]$$

$$D_{eff} = \frac{-J \cdot L \cdot R \cdot T}{A \cdot \Delta C \cdot z \cdot F \cdot \Delta E} \quad [23]$$

Where apart from the usual symbols;
T = absolute temperature [K]
R = gas constant = 8.3145 J/K·mol
Z = the charge of the diffusion ion (-1 for chloride)
F = Faradays constant = 96,485 A·s/mol
ΔE = effective potential drop over the specimen from the imposed potential ΔU [V or J/A·s]

Diffusion **into** (non-steady state flow) a porous media like concrete can be modelled by Fick's 2nd law of diffusion for one dimension;

$$\frac{\delta C}{\delta t} = D \cdot \frac{\delta^2 C}{\delta x^2} \quad [24]$$

where
C = molecule concentration
t = exposure time
D = diffusion coefficient
x = distance from exposed surface

Considering a *constant* diffusion coefficient over the diffusion period, an analytical solution of Eq. 24 has the form

$$C(x,t) = C_s - (C_s - C_i) \cdot erf \cdot \frac{x}{2\sqrt{D \cdot t}} \quad [25]$$

where

$C(x,t)$ = gas or liquid concentration in the concrete
C_s = gas or liquid concentration in the environment
erf = the error function

An experimental set-up for measuring chloride diffusivity under non-steady state condition is described in NT Build 443 where a concrete cylinder simply is submersed in a sodium chloride solution and the chloride profile as function of distance from exposed surface is measured at a given exposure time and fitted towards Eq. 25.

The diffusion coefficient D, depends among other things on:

- Porosity
- Amount of cracks, crack widths and crack depths
- w/c ratio
- Type of cement
- Degree of hydration
- Content of pozzolana
- Exposure time, see Eq. 26
- Temperature, see Eq. 27

Note that several of the preceding factors are strongly coupled. For instance will increased **w/c** ratio mean increased **porosity**. In non-steady state diffusion is it worth noting that the diffusion profile will be influenced by any concentration dependent adsorption or bonding of

the diffusing species, while this is NOT the case for steady state diffusion as the bonding presumably is saturated when the steady state conditions are achieved. Thus, steady state testing is preferred as diffusion indicator when comparing systems of different chemical composition.

Diffusion coefficients for concrete at different exposure times are often found to be well predicted by (i.e. diffusion coefficient decreases as the degree of hydration increases with time):

$$D_{ti} = D_{t0} \cdot (t_0 / t_i)^{\alpha} \quad [26]$$

where
D_{ti} = the diffusion coefficient at time t_i
D_{t0} = the diffusion coefficient at time t_0
α = aging parameter between 0 and 1, dependent on concrete and environment, meaning that the concrete becomes less permeable over time and that the apparent D at a given time is the integral of Ds over the diffusion period.

The diffusion coefficient at different temperatures is often found to be well predicted by

$$D_{T2} = D_{T1} \cdot e^{\frac{E_A}{R} \cdot \left(\frac{1}{T1} - \frac{1}{T2} \right)} \quad [27]$$

where
D_{T1} = the diffusion coefficient at absolute temperature T1
D_{T2} = the diffusion coefficient absolute temperature T2
E_A = the activation energy for diffusion [J/mol]

Thus, to be able to compare the effect of particle packing on diffusivity it is of importance to test mature samples so the degree of hydration is comparable and at the same temperature. Note that in the electromigration test, the temperature in the sample may rise differently depending on the resistivity of the material if the applied electrical potential is too high. NT Build 492 is describing a non-steady state electromigration method to achieve chloride diffusion coefficient, but Sengul and Gjørv (2008) recently showed that there is a linear correlation between obtained diffusion coefficients by this method and simply electrical conductivity.

The diffusion equations also apply for gases, and for instance Sercombe et al (2006) have made a thorough discussion of gas diffusion in cement pastes. Their experimental set-up for steady-state gas diffusion is reproduced in Fig. 15.

3.3.2 Permeation

Permeability is the ability of fluids and gases to flow through porous media like concrete under the influence of a constant pressure difference over the specimen. D'Arcy's law, see Eq. 28, is a simple proportional relationship between the instantaneous discharge rate through a porous medium (also called flux), the viscosity of the fluid and the pressure drop over a given media thickness.

$$Q = \frac{-\kappa \cdot A}{\mu} \cdot \frac{(P_b - P_a)}{L} \quad [28]$$

where
Q = total discharge [m^3/s]
κ = permeability coefficient [m^2]

($P_b - P_a$) = constant pressure drop [Pa = N/m^2 = kg/m·s^2]
μ = the dynamic viscosity of the fluid [kg/m·s]
L = length the pressure drop is taking place over (e.g. wall thickness) [m]
A = area of penetrated medium perpendicular to the direction of Q [m^2]

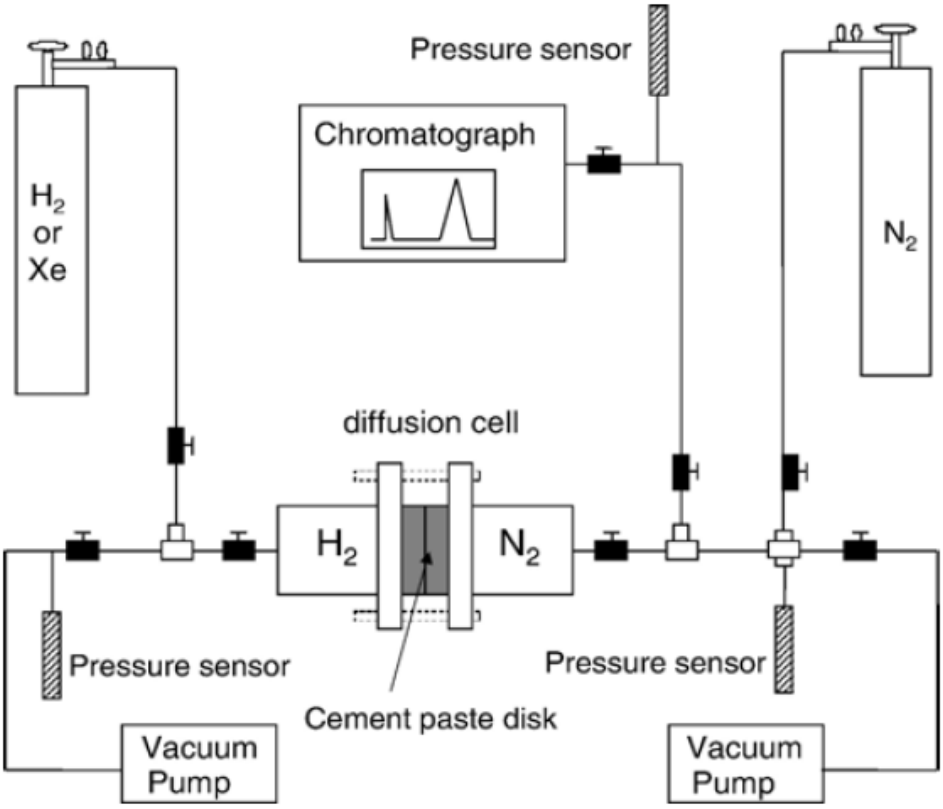

Fig. 15 Example for experimental set-up of steady state gas diffusion measurements after Sercombe et al (2007).

Darcy's law is a simple mathematical statement which neatly summarizes several familiar properties, including:

- if there is no pressure gradient over a distance, no flow occurs (this is hydrostatic conditions),
- if there is a pressure gradient, flow will occur from high pressure towards low pressure (opposite the direction of increasing gradient - hence the negative sign in Darcy's law),
- the greater the pressure gradient (through the same material), the greater the discharge rate, and
- the discharge rate of fluid will often be different — through different materials (or even through the same material, in a different direction) — even if the same pressure gradient exists in both cases.

A typical permeation experimental set up is shown in Fig. 16 for water permeation (Ye, 2005) and in Fig 17 for gas permeation after Lafhaj et al (2006).

.

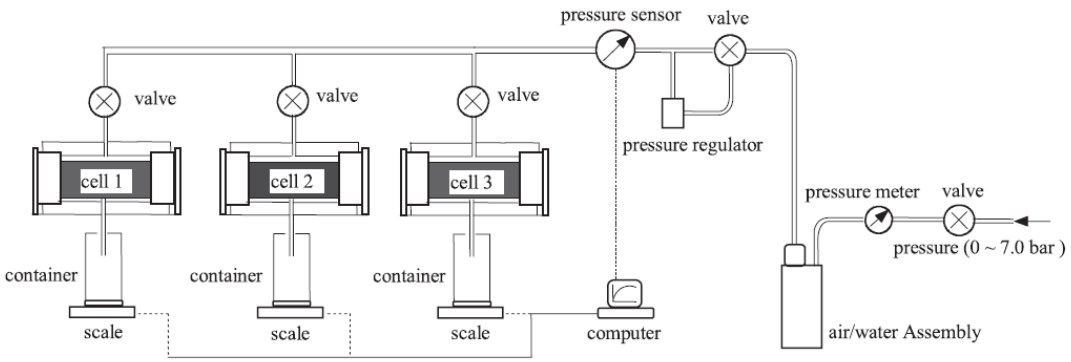

Fig. 16 Example for experimental set-up for water permeation after Ye (2005)

Note that permeability of a concrete is dependent on how it is prepared before tested. As Lydon (1995) pointed out for nitrogen permeation, the permeability coefficient can increase 7-fold if the sample is dried at 105°C in an oven versus dried at 20°C in air for 7 days water cured specimen or about double for concrete dried at 105°C versus 50°C for 56 days water cured specimens.

The permeability of cementitious materials to gas is also very dependent on the moisture state of the connected pore system as pointed out by Lafhaj et al (2006) in their attempt to correlate porosity, permeability and ultrasonic parameters of mortar with variable w/c and water content. The gas permeability versus porosity reproduced in Fig. 18 for fully saturated (FS), partially saturated (PS) and dry (D) specimens speaks for itself.

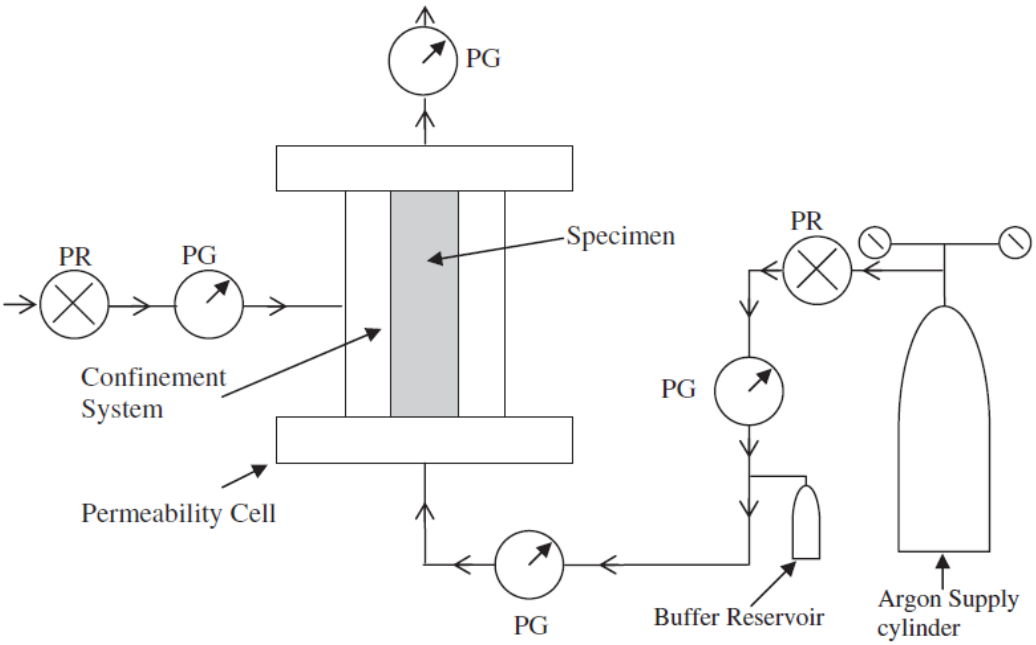

Fig. 17 Example for experimental set-up for gas permeation after Lafhaj et al (2006).

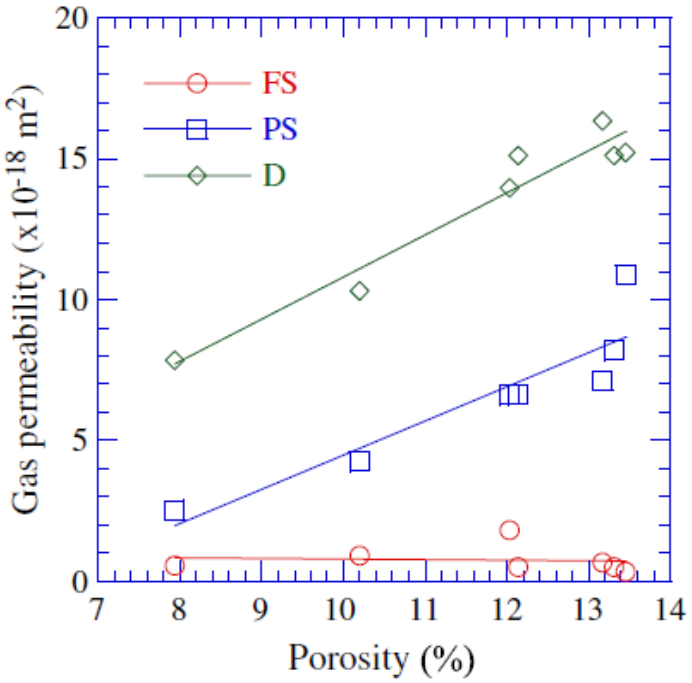

Fig. 18 Variation of gas permeability versus porosity of mortar and degree of pore saturation by water (Lafhaj, 2006).

3.3.3 Effects of pore characteristics on diffusion or permeation

Halamickova et al (1995) studied the influence of critical pore diameter as determined by mercury intrusion porosimetry (MIP) on chloride diffusion and water permeation of mortars. They found that the coefficient of chloride ion diffusion obtained by rapid electromigration test increased linearly with increasing critical pore diameter, while the water permeation coefficient increase followed a power law versus critical pore diameter.

Hedenblad (1997) measured the water vapour diffusion through cement paste in equilibrium with different relative humidity (RH) by a “cup method” as the diffusion depends both on porosity and RH. He managed to find an empirical relation between water vapour diffusion (although he called it permeability) and porosity.

4 PARTICLE PACKING AND CEMENT HYDRATION MODELS

4.1 Introduction

It is not the objective of this report to explain all particle packing and cement hydration models in their mathematical details, but merely give a short description of the principles for the most common ones. The details can otherwise be found in the referred publications for each of the models.

4.2 Optimal particle packing by solid suspension model (SSM)

De Larrard and Sedran (1994) utilized the concept of high packing density as a key for obtaining ultra-high-performance cementitious materials. Firstly, they applied two models allowing prediction of the packing density of a particle mix. These models were derived from the Mooney's suspension viscosity model. Secondly, considerations on the parameter to be maximized during the mix-design process were selected. Reference was made to the Maximum Paste Thickness concept, which led to the choice of fine sand for optimizing the compressive strength of cementitious materials. Then, an optimal material was sought, based on the following requirements: fluid consistency, classical components (i.e. ordinary aggregate, sand, Portland cement, silica fume, superplasticizer, water), and moderate thermal curing. A selection of mixes was made with the help of the Solid Suspension Model (SSM), and tests were performed in order to verify that the mix obtained definitely was optimal. Their final result was the production of a fluid mortar having a water/binder ratio of 0.14 and a compressive strength of 236 MPa. Even though their objective was castable mortar with high strength, it would inevitably lead to a mortar with very low permeability.

4.3 3D Microstructural simulation of cement paste (HYMOSTRUC3D)

The 3D microstructure of cement paste can be simulated and analyzed with the HYMOSTRUC3D model (Initiated by van Breugel, 1991, and further developed by Ye, 2004). In the HYMOSTRUC3D model, the hydration of cement paste is simulated as a function of the particle size distribution and the chemical composition of the cement, the w/c ratio and the reaction temperature. The model starts from the cement particle size distribution in a 3D body, where the cement particles are represented by spheres. Upon contact with water, and based on an interaction–expansion mechanism, the cement grains gradually grow. With progress of the reaction process, the growing particles become more and more connected. In this way, a simulated porous microstructure is formed. Fig. 19 shows an example of a simulated pore structure of a cement paste with w/c ratio 0.4 and porosity, Φc, of 15%.

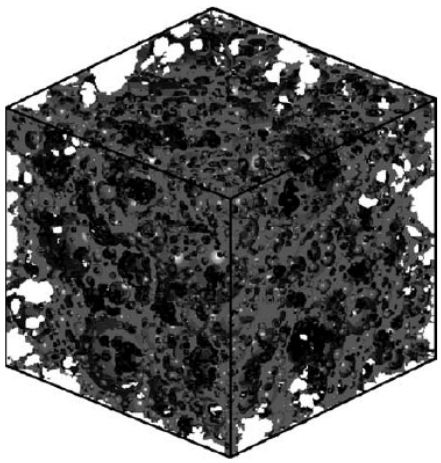

Fig. 19 3D simulated pore structure of cement paste with w/c = 0.40 and 15 % porosity (Ye, 2005).

To assess the connectivity and percolation of capillary porosity, a serial section algorithm associated with an overlap criterion is employed. The connectivity of the capillary pore network is thus obtained, and a link list pore network structure is built (see Fig. 20). The depercolation of capillary porosity is analyzed based on the connectivity of the capillary pore network. In the simulation, the effective porosity is obtained as the volume of the pores through which water flow can occur (see Fig. 20, block line). Detailed information on the geometrical and topological parameters of the simulated microstructure, such as porosity, effective porosity, pore size distribution and connectivity of pores, is obtained with the algorithm described by Ye et al (2003). The results, especially the connectivity of the capillary porosity, largely depend on both the image resolution of the slices (layers) and the layer depth. The layer depth is the distance between neighbouring slices, e.g., layers 0 and 1 at the left in Fig.20.

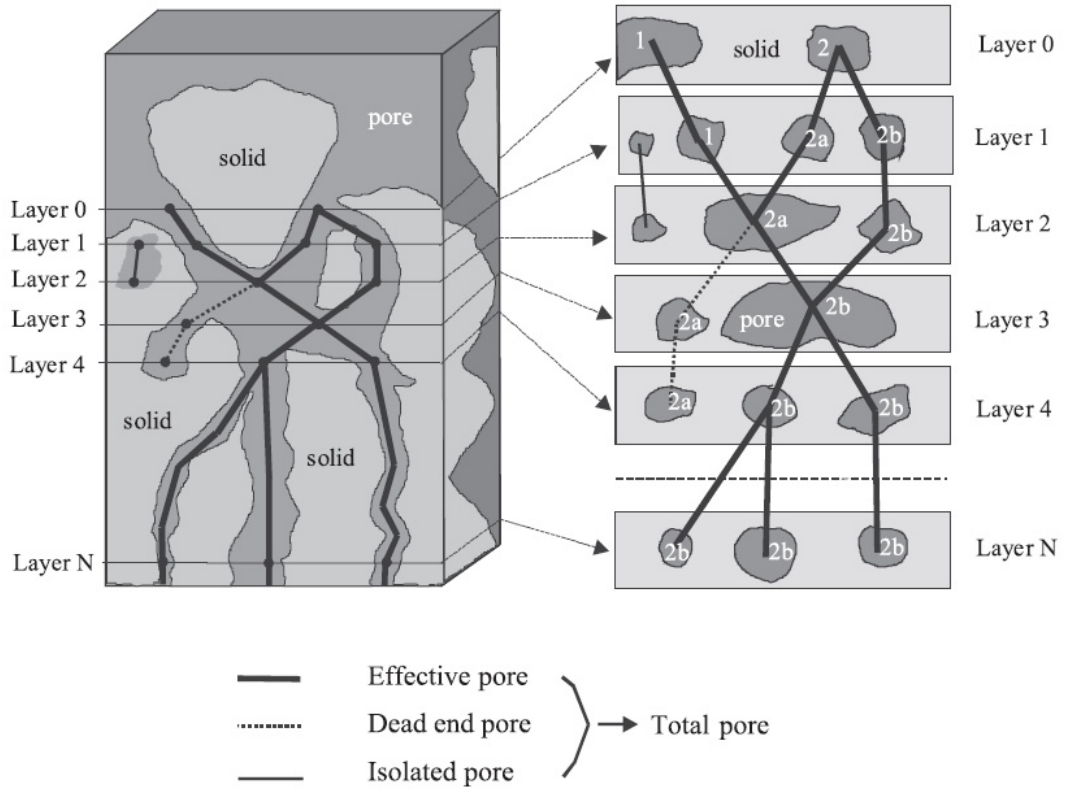

Fig. 20 Pore network structure determined by overlapping criteria; distinction between pores, dead-end pores and isolated pores (Ye, 2005).

4.4 The model of NIST; CEMHYD3D

The National Institute of Standards and Technology (NIST) in US has developed a computer model calculating the microstructure of hydrating cement in 3 dimensions, called CEMHYD3D (Bentz, 1997). This model also considers the chemistry of the cement and has lately been modified to take into account the reactivity of limestone.

The CEMHYD3D cement hydration model starts with a three-dimensional digital image of cement particles, and then uses cellular automation rules to simulate the reaction of cement with water and the development of cement paste microstructure. This stochastic model uses a digital image with a certain resolution to represent the reality of continuum shapes in a fairly small periodic unit cell. As such, it is potentially subjected to statistical fluctuation, finite size error, and the effects of digital resolution as discussed by Garboczi and Bentz (2001).

They evaluated the model in light of these potential sources of error, along with the effects of cement particle size distribution (PSD), water/cement (w/c) ratio, and cement chemistry, by focusing on the phase percolation and transport property predictions of the model. Statistical fluctuation and finite size error were shown to be of minor importance in the model. The effect of digital resolution was significant, however, but different from the case of a finite element or finite difference model. Unlike these cases, the ‘‘best’’ resolution is not necessarily the finest resolution, but must be chosen based on comparison with experiment and various physical length scales present in cement paste.

Chen and Brouwers (2008) modified the CEMHYD3D to improve the resolution problem (resolution versus computing time is a valid problem for all computer models).They showed that the effects of system resolution on the simulation results by CEMHYD3D mainly are due to the lack of considerations of the diffusion-controlled reactions in the model. A new concept (‘‘hydration layer”) was proposed for mitigating the effects of system resolution on the model predictions. By performing simulations with different system resolutions, Chen and Brouwers (2008) demonstrated the robustness of the improved model. They showed by comparing model predictions with experimental measurements that the use of hydration layer can successfully mitigate the bias brought by the system resolution.

More information on the CEMHYD3D model can be found in Benz (1997), Benz and Garboczi (1991), Garboczi and Benz (1991, 1992), Garboczi et al (1999).

Benz (2006) recently published a quantitative comparison of real and computer-generated (model) cement paste microstructures based on the analysis of three dimensional image sets by microtomography. In addition to a visual presentation of extracted two-dimensional images, the comparison was based on the calculation of the normalized two-point correlation function for a variety of phases including unhydrated cement, hydration products, and capillary porosity. A favourable comparison was observed between model and real microstructures for both the two-dimensional images and the computed correlation functions.

4.5 Software Package for Assessment of Compositional Evolution (SPACE)

The Software Package for the Assessment of Compositional Evolution (SPACE) consists of a two-stage simulation strategy, providing successively for the three-dimensional packing of a particulate system and the structural evolution, the latter representing a sintering, foaming, or hydrating particulate system. Hence, SPACE has versatile potentialities applied both on cement (Stroeven and Stroeven, 1999a) and to aggregate (Stroeven and Stroeven, 1999b). The initial distribution results from a generation process in which a predefined number of particles are dynamically mixed using a Newtonian motion model. Bulk material and interfaces can be simulated.

Stroeven and Stroeven (1999a) simulated cement hydration as an illustrative application of the SPACE system. The model starts with a simulated spatial distribution of anhydrous cement particles in a water-filled volume and simulates the hydration process through a series of relatively simple growth rules, which are iterated many times. The kinetic hydration model used here is similar to one used in HYMOSTRUC3D (section 4.3). The chemical reaction between cement and water results in expansion of the particle and in the formation of multiple contacts with other hydrating particles. The effects of this interparticle contact as well as the effect of water consumption on the hydration and expansion rate were explicitly accounted for, with the aid of a surface sampling method that can efficiently evaluate the degree of contact between particles. An example of how the calculations from the model can be presented is reproduced in Fig. 21, while a comparison between calculated strength versus hydration degree from the same model is shown in Fig. 22.

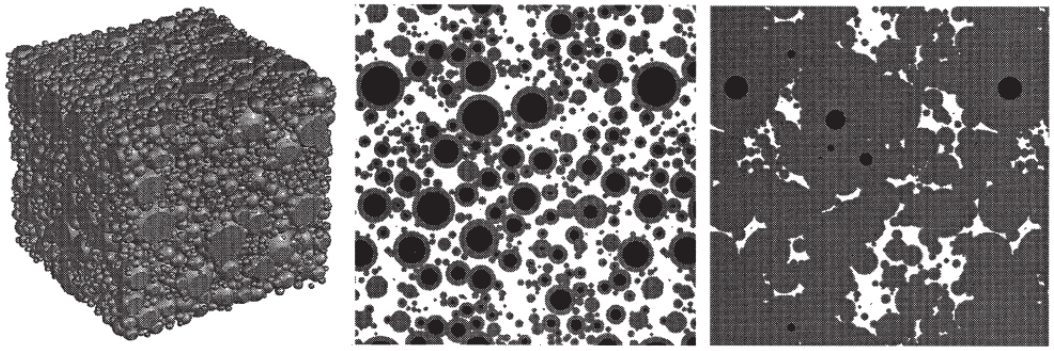

Fig. 21 (a) Three-dimensional view of hydrated cement paste and structure development as observed in a section plane after (b) 3.2 days and (c) 10 years of hydration. White areas indicate water and air, gray areas represent gel, and black areas correspond to unhydrated cement (from Stroeven and Stroeven, 1999a).

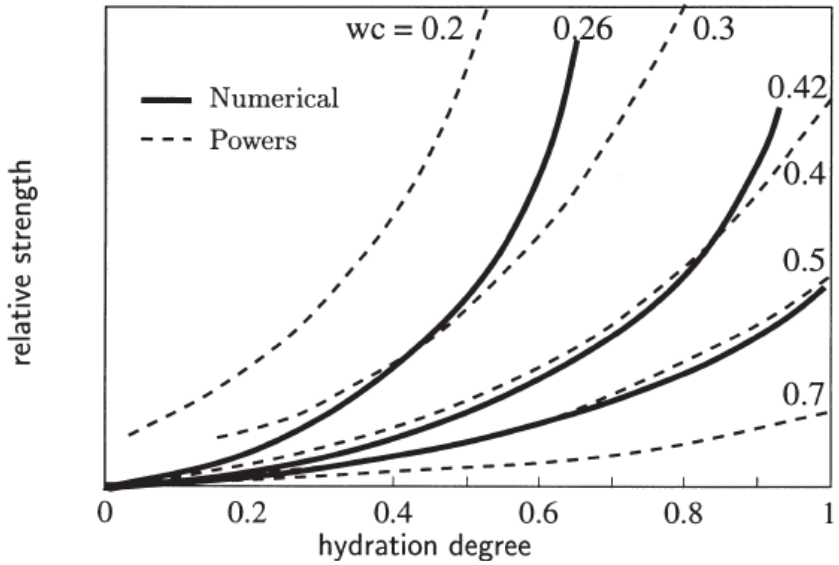

Fig. 22 Estimated relative strength as a function of the hydration degree (solid curves) vs. proposed curves by Locher (1976) as dashed curves.

4.6 Miscellaneous models

Navi and Pignant (1996) developed first a computer model for hydrating C_3S, which later was modified to cover cement hydration (Navi and Pignant, 1999).

Breysse and Gérard (1997) presented a micro-macro model predicting the water permeability of porous materials. The model is based on the concept of a hierarchical lattice. The model was first applied to mortars, but was extended and generalized to apply to cement paste and concrete. The model uses two phenomenological parameters; the effective porosity and tortuosity.

Delmi et al (2006) developed a mathematical model for predicting the coupled evolution of endogenous hydration and porosity of cement-based materials. The claimed originality was to take into account both the interactions between the hydration kinetics of the anhydrous compounds and between the evolution of the hydration rate and that of the porosity of the material. Through the scale change of the mass balance equations, the total porosity was related to the molar concentration of anhydrous compounds.

5 SPECIAL CEMENTITIOUS SYSTEMS

5.1 Low porosity cement

In 1972 an interesting concept of "Low porosity cement" was launched and extensively studied by Yudenfreund et al (1972a,b,c), Odler et al (1972a,b) and Brunauer et al (1973a,b). The concept consisted in regulating setting of gypsum-free cement clinker by the use of a mixture of lignosulphonate and alkali carbonate. In this way, paste of high fluidity could be obtained for very low w/c (down to 0.20) and hence low total porosity was obtained. It is uncertain whether the absence of Ettringite had a further positive effect in increasing the particle packing (see discussion in Chapter 2.5) or if the effect was solely obtained by the 0.5-1% dosage of dispersant (i.e. lignosulphonate). The knowledge of this system up to 1980 was summarized by Maage (1981).

Total porosities of paste with w/c = 0.20 was in the order of 16-22 vol% depending on the curing conditions for a degree of hydration 71-65%, which is about what is maximum achievable at such low w/c as pointed out by Yudenfreund et al (1972c). Another interesting aspect is that cement pastes with such a low w/c *expanded* several vol% when wet. The drying shrinkage of the pastes was also much lower than for OPC with more normal w/c (> 0.40).

Permeability is difficult to measure for cementitious materials with such a low porosity, but Maage (1981) referred to the permeability of low porosity cement paste being about one tenth of that of OPC paste. Concrete based on low porosity cement had about half the permeability coefficient of a good reference concrete, but the standard deviation was large.

5.2 Energetically modified cement

From the beginning of 1990s extensive study of the Energetically Modified Cement (EMC) produced by high intensive grinding/activation of ordinary portland cement (OPC) together with different types of fillers has been performed by Luleå University of Technology, EMC Development AB, Sweden, and SINTEF, Norway, as published by Ronin et al (1994, 1995, 1997a,b), Jonasson et al (1996) Rao et al (1997), Groth et al (1999), Hedlund et al (1999), Johansson et al (1999), Sellevold (1998), Ronin (2001) and Justnes et al (2005, 2006, 2007a,b,c).

Justnes et al (2007a) investigated the performance of concrete based on EMC where 20 (EMC-20) and 50% (EMC-50) of the cement was replaced with quartz sand and compared it to concrete based on OPC. This was done for equal water-binder ratios of 0.45, 0.50 and 0.60, and the chloride permeability (ASTM C 1202-94) is reproduced in Table 9, while the apparent and effective diffusion coefficients for chlorides obtained by steady state migration (NT Build 355) and non-steady state diffusion (NT Build 443) are plotted in Fig 23.

Table 9 Results from testing of chloride permeability according to ASTM C 1202 – 94)

Binder type	w/b-ratio	Average "Charge passed" in Coulombs±standard deviation	Evaluation of chloride permeability
OPC	0.45	3734±165	Moderate
	0.50	4030±135	High
	0.60	4828±448	High
EMC-50	0.45	763±62	Very Low
	0.50	821±39	Very Low
	0.60	976±106	Very Low
EMC-20	0.45	1271±141	Low
	0.50	1397±55	Low
	0.60	1649±185	Low

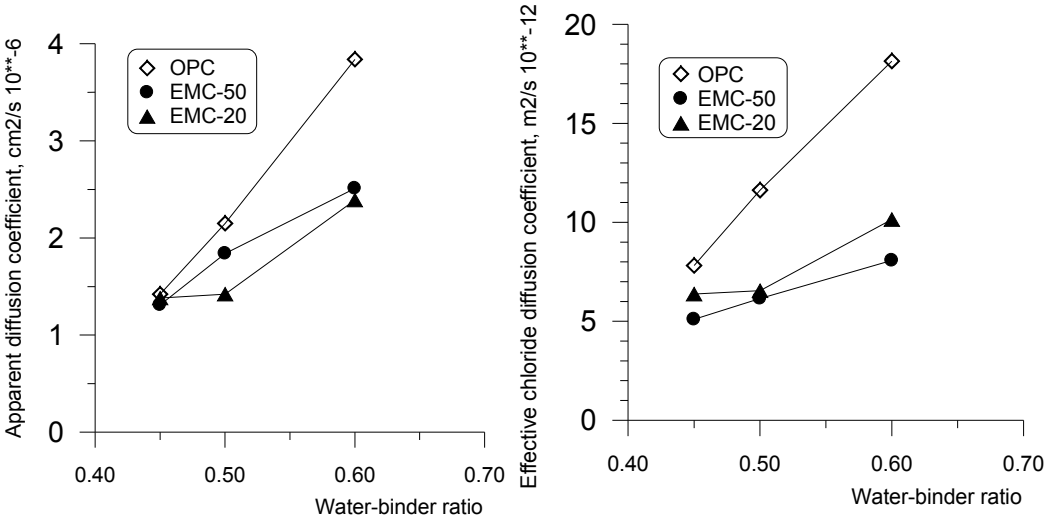

(a) Apparent Cl^- diffusion coefficient (b) Effective Cl^- diffusion coefficient

Fig. 23 Chloride ingress accelerated by electrical field under steady state conditions (a) and Cl^- concentration under non-steady state conditions (b) from Justnes et al (2007a).

The lower chloride diffusivity of the EMC samples compared to OPC is probably mainly due to finer particles in the EMC due to the intense grinding as well as potential improved packing. The result is finer pores already at time of setting as shown in Fig. 11. All concretes were water cured for 90 days prior to testing, so the degree of hydration should not be all that different. Sealed cured EMC-50 and OPC paste both achieved 76% hydration according to Justnes et al (2007a). The lowering effect on diffusion by EMC treatment relative to OPC seems to be larger for larger water-binder ratio.

Justnes et al (2007a) also tested capillary suction of water and water vapour diffusion for the same concretes and found increased resistance towards capillary suction and decreased water vapour diffusion coefficients for concrete based on EMC compared to OPC concrete.

5.3 Reactive powder concrete (RPC)

Reactive powder concretes (RPCs) form a new generation of ultrahigh performance concretes (UHPCs) according to Richard and Cheyrezy (1995). In RPCs, the enhancement of the homogeneity is obtained by the elimination of coarse aggregates, the densification of the mixture results from the optimization of the grain size distribution, the improvement of the microstructure is achieved by post-set heat treatment, and finally a high ductility is obtained by the incorporation of steel fibers (about 2 vol%).

Bonneau et al (2000) studied the granular packing and percolation threshold of RPC. Their RPC was composed of high cement content (730 kg/m^3), silica fume (240 kg/m^3) and very fine powders: sand (1,040 kg/m^3) and crushed quartz (220 kg/m^3), all aggregate with particle sizes comprised between 300 and 0.02 mm, and a low water content (w/c = 0.20). Steel fibers were not used in their work since they could disturb their electrical conductivity measurements. Bonneau et al (2000) found that the pores become disconnected (percolation threshold) when the degree of hydration reached about 26%, and claimed that this was in agreement with the computer model of Benz and Garboczi (1991).

A comment by the author of the present report to the recipe of RPC of Bonneau et al (2000) is that a binder with 33% silica fume (SF) of cement mass does not need to be much

optimized in particle packing to get a low permeability. If one uses the densities of 3.15 and 2.20 g/cm^3 for cement and SF, respectively, one can see that SF reaches 47 vol% of the cement volume. Considering the much smaller individual particles (in average 0.15 μm) of SF relative to cement (in average 15 μm), it is likely that the cement will be dispersed in a "continuous" SF slurry and that the pore sizes initially will be dominated by packing of SF. Thus, a high volume fraction of a fine, reactive powder such as SF will lead to low permeability without any further "optimized particle packing". This is presumably what is utilized in similar commercial products under the trade names of Densite™ and Ceramite™.

Bonneau et al (2000) made a comparison of what degree of hydration that was required to make pores disconnected in ordinary concrete (OC), high strength concrete (HSC) and reactive powder concrete (RPC) as reproduced in Table 10.

Table 10 Degree of hydration (α) and amount of hydrated cement to make porosity disconnected in various concretes.

Concrete type	Cement content (kg/m^3)	w/c	α	Hydrated cement (kg/m^3)	Reference
Ordinary (OC)	280	0.60	>1.00[a]	>280	Vernet et al (1998)
High strength (HSC)	420	0.33	0.54	226	Vernet et al (1998)
Reactive powder (RPC)	700	0.20	0.26	182	Bonneau et al (2000)

[a] α > 100% is of course impossible, so it means that pores will never be disconnected.

5.4 Multiple powder blends

Khan (2003) investigated the development of a high performance-low environmental impact concrete utilising blends of pozzolanic by-product materials as cement replacing materials. Pulverised fly ash (PFA) and Silica fume (SF) were used in ternary systems with the aim of exploiting the potential synergy between these materials, thus reducing or eliminating limitations inherent in individual materials. Compressive strength, oxygen permeability and porosity results at various ages are reported. Mortar containing 0%, 20%, 30% and 40% PFA to which 0%, 5%, 10% and 15% SF were incorporated as partial cement replacements, for the preparation of various combinations of ternary blended cement. A water-binder ratio of 0.27 was used throughout. Based on the experimentally obtained results, prediction models were developed. These enabled the establishment of iso-response contours showing the interaction between the parameters investigated. It was found that *the incorporation of 8–12% SF as cement replacement yielded the optimum performance, resulting in the lowest permeability and porosity values for all levels of PFA*. This investigation is another indication that a high amount of a fine, reactive powder will govern the permeability.

6 Future research

It appears like the fineness of the particles is determining the size of the pore openings governing the pore connectivity and thereby permeability if they are added in large enough quantities to disperse the coarser ones, which is obvious from the discussion of basic particle packing in Chapter 2.1. For a more normally distributed multiple particle composition, a wider particle size distribution is more beneficial to obtain optimize particle packing. Thus, making smallest possible reacting particles would give the ultimate low pore opening size if they are added in a sufficiently large quantity relative to the cement. The challenge is then to make them in the most economical way (grinding is expensive and limited to a certain size) and at the same time not let them hamper workability by being too reactive in the fresh state. Thus, the fine tail of PSD for e.g. a ternary cement should consist of slowly reacting particles; for instance nano-sized calcium carbonate made from precipitation reactions, clay calcined below sintering temperature that easily can be ground to 3 μm or perhaps fine recycled glass powder.

Further research is recommended for particle blends of fine calcium carbonate that will react with the pozzolanic reaction products of alumina-containing supplementary cementing minerals like fly ash or calcined clay for lowest possible permeability/diffusivity and thereby improved durability. Such combinations should not be limited to ternary blended cements, but also as a combination of concrete additives to the mixer or as pre-packed mortars for special applications.

During the review in this report, indications have been found that the initial Ettringite formation in the fresh state can hamper particle packing. Thus, efforts should be made to find alternatives to gypsum as setting regulator for cement and to see if the particle packing in such a case would be better. Another advantage of gypsum free Portland cement is that one potentially could allow concrete with such cement to cure above 70°C without the risk of delayed Ettringite formation. In such a case this could open up for increased productivity in the element production industry and save cost for cooling efforts in massive structures, albeit the risk of thermal cracks would not be removed.

In the discussion on how to measure particle packing in the fresh state, the method of centrifugal consolidation (section 3.1.7) seems most promising due its simplicity, quick result and operator independency. Thus, it is recommended to investigate this methodology further.

7 CONCLUSIONS

This State-of-the-Art report (STAR) gives an overview over factors influencing particle packing and porosity. An overview of methods for measuring and modelling particle packing and porosity is also made. Improved particle packing of the concrete matrix (i.e. particles < 125 μm) will reduce porosity and permeability of concrete and thereby improve durability of concrete. The findings are based on literature reviews.

It appears like the fineness of the particles is determining the size of the pore openings governing the pore connectivity and thereby permeability if they are added in large enough quantities to disperse the coarser ones, which is obvious from basic particle packing theory. For a more normally distributed multiple particle composition, a wider particle size distribution is more beneficial to obtain optimize particle packing. Thus, making smallest possible reacting particles would give the ultimate low pore opening size if they are added in a sufficiently large quantity relative to the cement. An excess of fine particles dispersing coarse ones (e.g. high dosage of silica fume relative to cement) can dominate the permeability all together, without being the result of a refined complex particle packing.

It is also demonstrated that it is not only the initial packing of particles, but also the increased volume of their solid reaction products that reduces permeability. Even particles considered by many to be inert (like limestone powder) will react when given sufficient reactants (e.g. calcium alumina hydrates from pozzolanic reaction of fly ash) and contribute positively to reduced permeability in theory.

Thus, making a powder fraction consisting of smallest possible reacting particles would give the ultimate low pore opening size if added in sufficient amount. The challenge is then to make them in the most economical way (grinding is expensive and limited to a certain size) and at the same time not let them hamper workability by being too reactive in the fresh state. Thus, the fine tail of particle size distributions consisting e.g. of a ternary cement should consist of slowly reacting particles; for instance nano-sized calcium carbonate made from precipitation reactions, clay calcined below sintering temperature that easily can be ground to 3 μm or perhaps fine recycled glass powder.

The most important parameters governing permeability and percolation of a concrete matrix seems to be pore connectivity and critical pore opening. There are indications showing that a concrete matrix will depercolate at a total porosity of 18-20 vol% independently of being obtained by low water-to-cement ratio, particle packing, degree of hydration etc.

When permeability of concrete matrix is lower than the whole concrete, it is pointed out that the permeability of the actual normal density aggregate may be higher than a well cured cementitious paste, and that the permeability increase observed for concrete not necessarily is due to a more porous interfacial zone between aggregate and matrix that many authors seem to focus on.

8 REFERENCES

Atahan, H.N., Oktar, O.N. and Taşdemir, M.A.: "Effects of water-to-cement ratio and curing time on the critical pore width of hardened cement paste", Construction and Building Materials, Vol. 23 (2009) pp. 1196-1200.

Banthia, N. and Mindess, S.: "Permeability measurements on cement paste", Proc. Material Research Society Symposium, Pore Structure and Permeability of Cementitious Materials, vol. 137, 1988, pp. 173–178, Pittsburgh.

Barnes, H.A. et al.: "An Introduction to Rheology", Elsevier Science B.V., Amsterdam, 1989, p. 122.

Benz, D.P.: "CEMHYD3D; a Three Dimensional Cement Hydration and Microstructure Development Modelling Package", Version 2.0 NISTIR 6845, US Department of Commerce, Washington DC, 1997 and also "Three-dimensional computer simulation of portland cement hydration and microstructure development", J. Am. Ceram. Soc., Vol. 80 (1997) pp. 3 – 21.

Bentz, D.P.: "Fibers, percolation, and spalling of high performance concrete", ACI Mater. J. Vol. 97 (3) (2000) pp. 351– 359.

Benz, D.P.: "Quantitative comparison of Real and CEMHYD3D Model Microstructures using correlation functions", Cement and Concrete Research, Vol. 36 (2006) pp. 259-263.

Benz, D. and Garboczi, E.: "Percolation of Phases in a Three-dimensional Cement Paste Microstructure Model", Cement and Concrete Research, Vol. 21 (1991), No. 2, pp. 325-344.

Bonneau, O., Vernet, C., Moranville, M. and Aïtcin, P.-C.: "Characterization of the Granular Packing and Percolation Threshold of Reactive Powder Concrete", Cement and Concrete Research, Vol. 30 (2000) pp. 1861-1867.

Breysse, D. and Gérard, B.: "Modelling of Permeability in Cement-based Materials: Part 1 - Uncracked Medium", Cement and Concrete Research, Vol. 27, No. 5 (1997) pp. 761-755.

Brunauer, S., Yudenfreund, M., Odler, I. and Skalny, J.: „Hardened Portland Cement Paste of Low Porosity. VI. Mechanism of the Hydration Process", Cement and Concrete Research, Vol. 3 (1973a) pp. 129-147.

Brunauer, S., Odler, I., Skalny, J. and Yudenfreund, M.: „Hardened Portland Cement Paste of Low Porosity. VII. Further Remarks about Early Hydration. Composition and Surface Area of Tobermorite Gel. Summary", Cement and Concrete Research, Vol. 3 (1973b), pp. 279-293.

Chen, W. and Brouwers, H.J.H.: "Mitigating the effects of system resolution on computer simulation of Portland Cement Hydration", Cement and Concrete Composites, Vol. 30 (2008) pp. 779-787.

Cody, A.M., Lee, H., Cody, R.D. and Spry, P.G.: "The Effects of Chemical Environment on the Nucleation, Growth and Stability of Ettringite $[Ca_3Al(OH)_6]_2(SO_4)_3 \cdot 26H_2O$", Cement and Concrete Research, Vol. 34 (2004) pp. 869-881.

Copeland, L.E. and Hayes, J.C.: "The determination of non-evaporable water in hardened Portland cement paste", ASTM Bulletin No. 194, Dec. 1953, pp. 70-74.

Cook, R.A. and Hover, K.C.: "Mercury Porosimetry of Hardened Cement Pastes", Cement and Concrete Research, Vol. 29 (1999) pp. 933-943.

De Larrard, F. and Sedran, T.: "Optimization of Ultra-High-Performance Concrete by the Use of Packing Model", Cement and Concrete Research, Vol. 24 (1994), pp 997-1009.

De Weerdt, K.: "Wet Particle Packing with Krieger Dougherty", Chicago, 2008

De Weerdt, K. and Justnes, H.: "Microstructure of the binder from the pozzolanic reaction between lime and siliceous fly ash, and the effect of limestone addition", Proceedings of the 1st International Conference on Microstructural Related Durability of Cementitious Composites, 13-15 October 2008a, Nanjing, China, pp. 107-116, RILEM Proceedings PRO 61, Edited by Wei Sun et al., ISBN 978-2-35158-066-0.

Delmi, M.M.Y., Aït-Mokhtar, A. and Amiri, O.: "Modelling the Coupled Evolution of Hydration and Porosity of Cement-based Materials", Construction and Building Materials, Vol. 20 (2006) pp. 504-514.

Forss, B.: "F-cement, a new low-porosity slag cement", Silicates Industriels, Vol. 48, No. 3, 1983, pp. 79-82.

Gallucci, E., Scrivener, K., Groso, K., Stampanoni, M. And Margaritondo, G.: "3D Experimental Investigation of the Microstructure of Cement Paste using Synchrotron X-ray Microtomography (μCT)", Cement and Concrete Research, Vol. 37 (2007) pp 360-368.

Garboczi, E.J. and Bentz, D.P: "Fundamental computer simulation models for cement-based materials", in: J. Skalny (Ed.), Materials Science of Concrete vol. II, American Ceramics Society, Westerville, OH, 1991, pp. 249– 277.

Garboczi, E.J. and Bentz, D.P.: "Computer simulation of the diffusivity of cement-based materials", J. Mater. Sci., Vol. 27 (1992) pp. 2083– 2092.

Garboczi, E.J., Bentz, D.P. and Martys, N.S.: "Digital imaging and pore morphology", in: P. Wong (Ed.), Methods in the Physics of Porous Media, Academic Press, San Diego, 1999, pp. 1– 41.

Garboczi, E.J. and Bentz, D.P.: "The effect of statistical fluctuation, finite size error, and digital resolution on the phase percolation and transport properties of the NIST cement hydration model", Cement and Concrete Research, Vol. 31, (10) (2001), pp. 1501–1514.

Groth, P. and Ronin, V.: "Influence of Energetically Modified Cement on Interfacial Bond and Fracture Toughness in Cement-Based Fibre Reinforced Composites", 5th International Symposium on Utilization of High Strength/High Performance Cement, Sandefjord 20-24 June 1999, Ed. by I. Holand and E. J. Sellevold, Norwegian Concrete Association, Oslo 1999, pp 1114- 1123, ISBN 82-91341-25-7.

Halamickova, P., Detwiler, R.J., Bentz, D.P. and Garboczi, E.J.: "Water Permeability and Chloride Ion Diffusion in Portland Cement Mortars; Relationship to Sand Content and Critical Pore Diameter", Cement and Concrete Research, Vol. 25, No. 4 (1995) pp. 790-802.

Hedenblad, G.: "The Use of Mercury Intrusion Porosimetry or Helium Porosity to Predict the Moisture Transport Properties of Hardened Cement Paste", Adv. Cem. Bas. Mat., Vol. 6 (1997) pp. 123-129.

Hillel, D.: "Soil and Water, Physical Principles and Processes", Academic Press, New York, 1971.

Hedlund, H., Ronin, V. and Jonasson, J.-E.: "Ecological Effective High Performance Cement Based Binders", 5th International Symposium on Utilization of High Strength/High Performance Cement, Sandefjord 20-24 June 1999, Ed. by I. Holand and E. J. Sellevold, Norwegian Concrete Association, Oslo 1999, pp. 1144-1153, ISBN 82-91341-25-7.

Hooton, R.D.: "What is needed in a permeability test for evaluation of concrete quality", Proc. Material Research Society Symposium, Pore Structure and Permeability of Cementitious Materials, vol. 137, Materials Research Society, Pittsburgh, 1988, pp. 141–150.

Johansson, K., Larsson, C., Antzutkin, O. N., Forsling, W., Rao, K. H. and Ronin V.: "Kinetics of the hydration reactions in the cement paste with mechanochemically modified cement ^{29}Si magic-angle-spinning NMR study", Cement and Concrete Research 29 (1999) pp. 1575-1581.

Jonasson, J.-E., Ronin, V. and Hedlund, H.: "High strength concrete with energetically modified cement and modelling of shrinkage caused by self-desiccation", Proceedings of the 4th International Symposium on the Utilization of High Strength/High Performance Concrete, Paris, France, August 1996, Presses Pont et Chausses, Paris, 1996, pp. 245-254.

Justnes, H.: "Thaumasite formed by sulfate attack on mortar with limestone filler" Cement and Concrete Composites Journal, Vol. 25, Dec. 2003, pp. 955-959.

Justnes, H.: "Silica Fume in High-Quality Concrete - A Review of Mechanism and Performance", Proceedings of the 9th CANMET/ACI International Conference on Fly Ash, Silica Fume, Slag and Natural Pozzolans in Concrete, ACI SP-242, Ed. Mohan Malhotra, Warszawa, Poland, 21-25th May, 2007, SP-242-6, pp. 63-78.

Justnes, H. and Kjellsen, K.O.: " Bulk Structure of CSH from C_3S/Alite Hydration as a Function of Time", Extended Abstracts from the Cement and Concrete Science Seminar organized by The Institute of Materials, Minerals and Mining, Dept. Civil Engineering and Materials, University of Leeds, Leeds, UK, 8-9th September 2003, 4 pp.

Justnes, H. and Rodum, E.: "Case Studies of Thaumasite Formation", Proceedings of the 7th CANMET/ACI International Conference on Durability of Concrete", Montreal, Canada, May 28 – June 3, 2006, ACI SP-234-33, pp. 521-537.

Justnes, H. and Vikan, H.. "Viscosity of Cement Slurries as a Function of Solids Content", Annual Transactions of the Nordic Rheology Society, Vol. 13, the Nordic Rheology Conference, Tampere, Finland, June 1-3, 2005, pp. 75-82

Justnes, H., Van Dooren, M., Van Gemert, D.: "Reasons for Workability Loss in Cementitious Binders", 7th CANMET/ACI Int. Conf. On Superplasticizers and Other Chemical Admixtures in Concrete, Berlin, Germany, October 2003, Supplementary Papers, pp. 53-65.

Justnes, H., Elfgren, L. and Ronin, L.: "Mechanism for Performance of Energetically Modified Cement versus Corresponding Blended Cement", Cement and Concrete Research, Vol. 35 (2005) pp. 315-323.

Justnes, H., Ronin, V. and Jonasson, J.-E.: "Performance of Energetically Modified Cement (EMC) and Highly Reactive Pozzolan based on Fly Ash", Proceedings of 6th International

Symposium on cement & Concrete (ISCC) and CANMET/ACI International Symposium on Concrete Technology for Sustainable Development, 19th-22nd September, 2006, Xi'an, China, Vol. 1, pp. 361-369 (paper no. 55).

Justnes, H., Dahl, P.A., Ronin, V., Jonasson, J.E. and Elfgren, L.: "Microstructure and Performance of Energetically Modified Cement (EMC) with High Filler Content", Cement and Concrete Composites, Vol. 29, 2007a, pp. 533-541.

Justnes, H., Ronin, V., Jonasson, J.-E. and Elfgren, L.: "Mechanochemical Technology: Synthesis of Energetically Modified Cements (EMC) with High Volume Fly ash Content", Proceedings of the 12th International Congress on the Chemistry of Cement, July 8 - 13, 2007b, Montreal, Canada, paper 84 (TH3-14.4) 12 pp.

Justnes, H., Ronin, V., Jonasson, J.-E. and Elfgren, L.: "Mechanochemical Technology: Energetically Modified Cements (EMC) with High Volume Quartz or Fly Ash", Proceedings of International Conference on Sustainability in the Cement and Concrete Industry, September 16-19, 2007c, Lillehammer, Norway, pp. 163 - 177.

Justnes, H., Wuyts, F. and Van Gemert, D.: "Hardening Retarders for Massive Concrete", Proceedings of 5th ACI/CANMET International Conference on High-Performance Concrete Structures and Materials, ACI SP-253-4, Manaus, Brazil, 18-20 June, 2008, pp. 41-56. (ISBN 978-0-8-87031-277-9).

Khan, M.I: "Iso-responses for strength, permeability and porosity of high performance mortar", Building and Environment, Vol. 38 (2003) pp. 1051 – 1056.

Krieger I. M. and Dougherty T. J.: "A mechanism for Non-Newtonian flow in Suspensions of Rigid Spheres", Trans. Soc. Rheol., 3 (1959), pp. 137-152.

Lafhaj, Z., Goueygou, M., Djerbi, A. and Kaczmarek, M.: "Correlation between Porosity, Permeability and Ultrasonic Parameters of Mortar with variable water/cement Ratio and Water Content", Cement and Concrete Research, Vol. 6 (2006) pp. 625-633.

De Larrard F.: "Concrete mixture proportioning, A scientific approach", EF & Spon, London, 1999.

Locher, F.W.: "The Effect of Hydrochloric Acid-Laden Vapours on Concrete and Other Building Materials (in German), Allianz-Bericht für Betriebstechnik und Schadenverhütung, No. 19 (1973) pp. 11-16.

Locher, F.W.: "Die Festigheit des zements", Beton, Vol. 26, No. 8 (1976) pp. 283-285.

Lothenbach, B., Matschei, T., Möschner, G. and Glasser, F.P.: „Thermodynamic Modelling of the Effect of Temperature on the Hydration and Porosity of Portland Cement", Cement and Concrete Research, Vol. 38 (2008), pp. 1-18.

Lydon, F.D.: "Effect of Coarse Aggregate and Water/Cement Ratio on Intrinsic Permeability of Concrete Subjected to Drying", Cement and Concrete Research, Vol. 25, No. 8 (1995) pp. 1737-1746.

Maage, M.: "Låg Porøsitet Betong - Statusrapport" (in New Norwegian), Report BML 81.201, January 1981, 25 pp., Institute of Building Materials, Norwegian University of Science and Technology, Trondheim, Norway.

Mansoutre, S., Colombet, P. and Van Damme, H. : "Water retention and granular rheological behaviour of fresh C_3S paste as a function of concentration". Cement and Concrete Research Vol. 29 (1999), pp. 1441-1453.

Marquardt I. "Ein Misschungskonzept für selbstverdichtenden Beton auf der Basis der Volumenkenngrössen und Wasseransprüche der Ausgangsstoffe". Rostock, Germany: Univ., Fak. für Ingenieurswissenschaften, Fachbereich Bauingenieurswesen, Fachgebiet Baustoffe, 2002. 190 pages {PhD Thesis in German}

Matschei, T., Lothenbach, B. and Glasser, F.P.: "The AFm phases in Portland cement", Cement and Concrete Research, Vol. 37, 2007a, pp. 118-130.

Matschei, T., Lothenbach, B. and Glasser, F.P.: "The role of calcium carbonate in cement hydration", Cement and Concrete Research, Vol. 37, 2007b, pp. 551-558.

Matschei, T., Lothenbach, B. and Glasser, F.P.: "Thermodynamic properties of Portland cement hydrates in the system $CaO-Al_2O_3-SiO_2-CaSO_4-CaCO_3-H_2O$", Cement and Concrete Research, Vol. 37, 2007c, pp. 1379-1410.

Mehta, P.K., Manmohan, C.: "Pore size distribution and permeability of hardened cement paste", 7th International Congress on the Chemistry of Cement, Paris, France, Vol. 3 (7) (1980) pp. 1 – 5.

Miller, K.T., Melant, R.M. and Zukoski, C.F.: "Comparison of the compressive yield response of aggregated suspensions: Pressure filtration, Centrifugation, and osmotic consolidation". Journal of the American Ceramic Society, Vol. 79, No. 10, pp. 2545-2556.

Navi, P and Pignant, C.: "Simulation of cement hydration and the connectivity of the capillary pore space", Adv. Cem. Based Mater., Vol. 4 (1996) pp. 58– 67.

Navi, P. and Pignant, C. "Three-dimensional characterization of the pore structure of a simulated cement paste", Cement and Concrete Research, Vol. 29 (4) (1999), pp. 507– 514.

NT Build 355: "Concrete, mortar and cement based materials: Chloride diffusion coefficients from migration cell experiments", Edition 2, approved 1997-11, 4 pages (Can be obtained through www.nordicinnovation.net).

NT Build 443: "Concrete, hardened: Accelerated chloride penetration", Approved 1995-11, 5 pages (Can be obtained through www.nordicinnovation.net).

NT Build 492: "Concrete, mortar and cement based repair materials. Chloride migration coefficient from non-steady state migration experiments", Approved 1999-11, 8 pp. (Can be obtained through www.nordicinnovation.net).

Odler, I., Hagymassy, J., Bodor, E.E., Yudenfreund, M. and Brunauer, S.: „Hardened Cement Pastes of Low Porosity. IV. Surface Area and Pore Structure", Cement and Concrete Research, Vol. 2 (1972b), pp. 577-589.

Odler, I., Yudenfreund, M., Skalny, J. and Brunauer, S.: „Hardened Cement Pastes of Low Porosity. III. Degree of Hydration. Expansion of Paste. Total Porosity.", Cement and Concrete Research, Vol. 2 (1972a) pp. 463-480.

Okamura, H. and Ozawa, K.: "Mix design for self-compacting concrete", Concrete library of the JSCE, No 25, 1995, pp. 107-120 (Translation from Proc. ISCE, no 496/v-24, 1994.8)

Powers, T.C.: "The Physical Structure and Engineering Properties of Concrete", PCA Res. Dept. Bull., 90 (1958).

Powers, T.C., Copeland, L.E., Hayes, J.C., Mann, H.M.: "Permeability of Cement Paste", J. Am. Concr. Inst. Proc. 51 (1954), pp. 285-298, or PCA Res. Dept. Bull. 53.

Powers, T.C., Copeland, L.E., Hayes, J.C. and Mann, H.M.: "Permeability of Portland cement paste", J. ACI, Vol. 51 (1955) pp. 285– 298.

Powers, T.C., Copeland, L.E., Mann, H.M.: "Capillary continuity or Discontinuity in Cement Pastes", J. PCA Res. Dev. Lab., Vol. 1 (1959) No. 2, pp. 38-48.

Puntke, W. : " Wasseranspruch von feinen Kornhauf-werken" (in German). Beton, Vol 52 (2002) No. 5, pp. 242–248

Rao, K. H., Ronin, V. and Forsberg, K. S. E.: "High performance energetically modified Portland blast-furnace cements", Proceedings of the 10th International Congress of the Chemistry of Cement (Ed. by H. Justnes), Gothenburg, June 1997. Inform Trycket AB, Gothenburg, 3ii104, 9 pp (ISBN 91-630-5497-5).

Regourd, M.: "Structure and behaviour of slag Portland cement hydrates", Proceedings of the 7th International Congress on the Chemistry of Cement, Paris, 1980, Vol. I, pp. III-2/10-III-2/26.

Richard, P. and Cheyrezy, M.: "Composition of Reactive Powder Concrete", Cement and Concrete Research, Vol. 25 (1995), No. 7, pp. 1501-1511.

Richartz, W.: "On the formation of the aluminous hydrate phases during setting of cement", Tonindustrie-Zeitung, Vol. 90, No. 10, 1966, pp. 449-457.

Ronin, V. and Jonasson, J.-E.: "Investigation of the effective winter concreting with the usage of energetically modified cement (EMC) - material science aspects". Report 1994:03, Div. Structural Engineering Luleå University of Technology, Luleå, Sweden, 1994, 24 pp.

Ronin, V, Jonasson, J-E.: "High strength and high performance concrete with use of EMC hardening at cold climate conditions", Proc. Int. Conf. Concrete under Severe Conditions, Sapporo, Japan, August 1995, pp.

Ronin, V., Jonasson, J.-E., and Hedlund, H.: "Advanced modification technologies of the Portland cement based binders for different high performance applications." Proceedings of the 10th International Congress on the Chemistry of Cement (Ed. by H. Justnes), Gothenburg, June 1997a. Inform Trycket AB, Gothenburg, 2ii077, 8 pp (ISBN 91-630-5496-5).

Ronin, V. et al: "Method for producing cement", European Patent EP 0 696 261 B1, 1997b, 13 pp.

Ronin, V.: "A method of treating cement clinker", European Patent EP 0 975 557 B1, 2001, 6 pp.

Schwartz, W.: "Novel Cement Matrices by Accelerated Hydration of the Ferrite Phase in Portland Cement via Chemical Activation: Kinetics and Cementitious Properties", Advances in Cement Based Materials, Vol. 2 (1995) pp. 189-200.

Sellevold, E. J.: "Summary and Evaluation of SINTEF test results on Energetically Modified Cements (EMC)", SINTEF, Report Number STF22 F98764, 1998-09-18, 8 pp.

Sengul, O. and Gjørv, O.E.: "Electrical Resistivity Measurements for Quality Control during Concrete Construction", ACI Materials Journal, Vol. 105 (2008) No. 6, pp. 541-547.

Sercombe, J., Vidal, R., Gallé, C. And Adenot, F.: "Experimental Study of Gas Diffusion in Cement Paste", Cement and Concrete Research, Vol. 37 (2007) pp. 579-588.

Smolczyk, H.-G.: "The hydration products of cements with high contents of blastfurnace slag", Zement-Kalk-Gips International, Vol. 18, No. 5, 1965, pp. 238-246.

Stauffer, D. and Aharony, A.: "Introduction to Percolation Theory", 2nd ed., Taylor and Francis, London, 1992.

Stroeven, M. and Stroeven, P.: "SPACE system for Simulation of Aggregated Matter Application to Cement Hydration", Cement and Concrete Research, Vol. 29 (1999a) pp. 1299-1304.

Stroeven, P. and Stroeven, M.: "Assessment of Packing Characteristics by Computer Simulation", Cement and Concrete Research, Vol. 29 (1999b) pp. 1201-1206.

Tangpagasit, J., Cheerarot, R., Jaturapitakkul and Kiattikomol, K.: "Packing Effect and Pozzolanic Reaction of Fly Ash in Mortar", Cement and Concrete Research, Vol. 35 (2005) pp. 1145-1151.

Uchikawa, H.: "Effect of blending components on hydration and structure formation", Proceedings of the 8th International Congress on the Chemistry of Cement, Rio de Janeiro, 1986, Vol. 1, pp. 249-280.

Van Breugel, K.: "Simulation of hydration and formation of structure in hardening cement-based materials", Dissertation, Delft University of Technology, The Netherlands, 1991.

Vernet, C., Lukasik, J. and Prat, E.: "Nanostructure, Porosity, Permeability and Diffusivity of Ultra-High performance Concrete", Proceedings of 1st International Symposium on HPC and RPC (Eds. P-C. Aïtcin and Y. Delagrave), Sherbrook, Canada, Vol. 3 (1998) pp. 17-36.

Wang, A., Zhang, C. and Zhang, N.: "Study on the Influence of the Particle Size Distribution on the Properties of cement", Cement and Concrete Research, Vol. 27 (1997) No. 5, pp. 685-695.

Wang, A., Zhang, C. and Zhang, N.: "The Theoretical Analysis of the Influence of the Particle Size Distribution of Cement System on the Property of Cement".

Yang, K., Zhang, C. and Liu, Z.: "The Influence of Calcium Lignosulphonate - Sodium Bicarbonate on the Status of Ettringite Crystallization in Fly Ash Cements", Cement and Concrete Research, Vol. 32 (2002) pp. 51-56.

Ye, G.: "Experimental study and numerical simulation of the development of the microstructure and permeability of cementitious materials." PhD thesis, Delft University of Technology, Delft, 2004.

Ye, G.: "Percolation of Capillary Pores in Hardening Cement Pastes", Cement and Concrete Research, Vol. 35 (2005) pp. 167-176.

Ye, G., van Breugel, K. and Fraaij, A.L.A.: "Three-dimensional microstructure analysis of numerically simulated cementitious materials", Cement and Concrete Research, Vol. 33 (2003) pp. 215– 222.

Ye, G., Lura, P., van Breugel, K. and Fraaij, A.L.A.: "Study on the development of the microstructure in cement-based materials by means of numerical simulation and ultrasonic pulse velocity measurement", Cement and Concrete Composites Vol. 26, No. 5 (2004) pp. 491-497.

Yudenfreund, M., Odler, I. and Brunauer, S.: „Hardened Cement Pastes of Low Porosity. I. Materials and Experimental Methods", Cement and Concrete Research, Vol. 2 (1972a) pp. 313-330.

Yudenfreund, M., Skalny, J., Raouf, Mikhail, R. Sh. and Brunauer, S.: „Hardened Cement Pastes of Low Porosity. II. Exploration Studies. Dimensional Changes", Cement and Concrete Research, Vol. 2 (1972b) pp. 331-348.

Yudenfreund, M., Hanna, K.M., Skalny, J., Raouf, Odler, I. and Brunauer, S.: „Hardened Cement Pastes of Low Porosity. V. Compressive Strength", Cement and Concrete Research, Vol. 2 (1972c) pp. 731-743.

SINTEF Building and Infrastructure is the third largest building research institute in Europe. Our objective is to promote environmentally friendly, cost-effective products and solutions within the built environment. SINTEF Building and Infrastructure is Norway's leading provider of research-based knowledge to the construction sector. Through our activity in research and development, we have established a unique platform for disseminating knowledge throughout a large part of the construction industry.

COIN – Concrete Innovation Center is a Center for Research based Innovation (CRI) initiated by the Research Council of Norway. The vision of COIN is creation of more attractive concrete buildings and constructions. The primary goal is to fulfill this vision by bringing the development a major leap forward by long-term research in close alliances with the industry regarding advanced materials, efficient construction techniques and new design concepts combined with more environmentally friendly material production.